



# Resilient biofuel supply chain network design under disruption risk and uncertainty considering parameter dependency: Iran case study

Mohammad Ali Karimi, Hossein Neghabi\*

Department of Industrial and Systems Engineering, Ferdowsi University of Mashhad, Mashhad, Iran

## ARTICLE INFO

### Keywords:

Biofuel supply chain  
Network design  
Robust optimization  
Stochastic programming  
Min-max regret  
Resilience

## ABSTRACT

This paper introduces three distinct models, stochastic, robust, and min-max regret models, for designing the biofuel supply chain network under conditions of biomass price uncertainty and disruptions that reduce the quantity of biofuel. The primary objective of this study, through the development of these models, is to offer a flexible framework that can be effectively adapted to various problem scenarios. These models are proposed to meet the specific needs of decision-makers while addressing different risks inherent in the problem. In contrast to previous related studies, this paper introduces a more realistic problem by considering the dependency of biomass prices on biomass availability, which is influenced by disruptions. An efficient algorithm incorporating the benders decomposition algorithm enhanced with acceleration technique is developed to alleviate the computational burden and reduce problem-solving time. Comprehensive experiments are conducted utilizing Iran's real case study to examine the concurrent influence of uncertainty and disruption on the biofuel supply chain network and assess the performance of the introduced models and algorithms. The results obtained from solving various test problems demonstrate that each model generates a unique structure for the biofuel supply chain network, with each structure being optimized to meet the specific conditions and requirements of the decision-makers. Furthermore, the findings underscore the effectiveness and computational efficiency of the proposed algorithm in addressing the problem at hand.

## 1. Introduction

The uncontrolled emission of greenhouse gases accelerates global warming, resulting in catastrophic environmental and human impacts (Sy et al., 2018). Extensive research and practical observations (Aboytes-Ojeda et al., 2022; Kazakçı et al., 2007; Sy et al., 2018) have demonstrated that substituting fossil fuels with biofuels can effectively reduce greenhouse gas emissions and control the impacts of global warming. Biofuels, obtained from organic sources such as crops, agricultural waste, and algae, are environmentally friendly substitutes for fossil fuels. Biofuels possess advantages such as worldwide availability, acceptable conversion efficiency, and CO<sub>2</sub>-neutral production and consumption (Zailan et al., 2021). The production and distribution of biofuels require an efficient and resilient biofuel supply chain (BSC) network. The BSC encompasses various components, including biomass suppliers, biofuel refineries, biomass and biofuel storage facilities, and customers. BSC network design problem involves making decisions on the location and capacity of production and storage facilities, selecting

suppliers, and allocating resources and customers (Fattahi and Govindan, 2018).

Biofuels can be used in the transportation sector, power generation, and other applications as vehicle fuel or incorporated as supplements to conventional petroleum-based fuels. Over the recent decades, many countries have been trying to expand their biofuel production facilities. Additionally, liquid biofuel production has increased significantly, with a 53 % rise observed during this period. The USA, Brazil, Indonesia, China, and Germany are the five leading countries in the production of biofuels. Additionally, at the same time, there has been a notable 67 % increase in global biofuel consumption. The USA and Brazil have emerged as prominent leaders in this domain, with 38 % and 23 % significant market shares, respectively, in overall biofuel consumption (Torroba and Productivo, 2020). Thailand, Germany, France, Japan, Iran, Argentina, and Colombia are among the countries actively pursuing the expansion of both the production and consumption of biofuels. This transition from fossil fuels to biofuels necessitates the development of integrated BSC networks.

\* Corresponding author at: Department of Industrial and Systems Engineering, Ferdowsi University of Mashhad, Azadi Square, Mashhad, Razavi Khorasan Province, Iran.

E-mail addresses: [mohammadali.karimihassanabadi@mail.um.ac.ir](mailto:mohammadali.karimihassanabadi@mail.um.ac.ir) (M.A. Karimi), [hosseinneghabi@um.ac.ir](mailto:hosseinneghabi@um.ac.ir) (H. Neghabi).

<https://doi.org/10.1016/j.compchemeng.2025.109267>

Received 18 January 2025; Received in revised form 17 June 2025; Accepted 26 June 2025

Available online 29 June 2025

0098-1354/© 2025 Elsevier Ltd. All rights are reserved, including those for text and data mining, AI training, and similar technologies.

This paper considers the BSC framework with a four-echelon structure, including biomass suppliers, biorefineries, biofuel storage facilities, and customers. Designing an efficient BSC network involves strategic decisions regarding determining the optimal number and location of biorefineries and storage facilities. Additionally, tactical decisions encompass allocation decisions and the identification of optimal routes for biomass and biofuel flow among the different facilities. In planning time horizon, problem parameters may deviate from the intended plan. For instance, disruptions such as floods, storms, pests, and frosts can significantly decrease biomass yield. Furthermore, the parameters of the problem fluctuate due to factors such as changes in economic and political conditions, as well as the instability in global fuel prices. Consequently, modeling and planning based on deterministic conditions can result in infeasible and costly solutions. Therefore, it is crucial to consider uncertainty and potential disruptions during the planning phase (Fattahi and Govindan, 2018).

The success of a BSC largely depends on its efficiency and resilience, both of which are significantly influenced by uncertainties and disruptions. These factors must be carefully considered during the design of the biomass supply chain. Fluctuations in parameters such as biomass yield, biomass price, customer demand, and biofuel price are categorized as operational risks or uncertainties. These operational risks, characterized by their high probability but low impact, can typically be mitigated through short-term decision-making strategies (Snoeck et al., 2019). In contrast, disruptions represent a distinct category of supply chain risks. These are low-probability but high-impact events whose effects cannot be effectively managed in the short term and require comprehensive medium- and long-term planning. Such disruptions include natural disasters, such as floods, earthquakes, storms, and severe climate changes, as well as human-induced events, such as fires and wars. These disruptions can result in the partial or complete shutdown of the supply chain, emphasizing the need for robust strategies to enhance the resilience of BSCs against such risk (Li et al., 2021). This paper presents a comprehensive BSC network design, addressing uncertainty and disruption. Specifically, it is assumed that disruptions affect biomass yield, which in turn influences the purchasing costs of biomass.

Stochastic programming and robust models are common approaches to designing an efficient and resilient BSC network under uncertainty and disruption. Stochastic programming is a risk-neutral modeling approach that accounts for the probabilistic nature of problem parameters, optimizing supply chain performance under uncertainty. This method effectively manages uncertain parameters and provides valuable insights into the supply chain's performance across different scenarios (Snoeck et al., 2019). In contrast, robust models adopt a risk-averse perspective and utilize diverse criteria to model problems (Bertsimas and Sim, 2004). A key advantage of some robust models is their ability to address uncertainties without relying on precise probability distribution functions for the uncertain parameters (Mulvey et al., 1995). This flexibility makes them particularly well-suited for situations where such distributions are unavailable (Ben-Tal et al., 2005). It allows decision-makers to design supply chains that maintain resilience and efficiency despite a broad range of potential uncertainties and disruptions (Ben-Tal et al., 2005; Zhao et al., 2021). Each modeling approach can lead to a different structural design for the BSC network. Therefore, selecting an appropriate mathematical model for designing the BSC network requires careful consideration of the problem's conditions and the decision-makers' objectives. This paper proposes three distinct mathematical models to address a broader range of BSC network design problems.

The first model, which belongs to the category of stochastic programming, assumes the availability of sufficient data and aims to minimize the expected costs of the BSC. The second model utilizes robust modeling techniques, assuming that historical data is available to predict the probability distribution of parameters. Its objective is to minimize the target threshold cost of the BSC while considering a specific confidence level. The third model, also categorized as a robust approach,

assumes that sufficient historical data to predict the probability distribution of parameters under disruption is unavailable. Its objective is to minimize the maximum regret, making it suitable for scenarios with severe disruption. These three models collectively offer a comprehensive framework for designing BSC under varying conditions and levels of uncertainty. In the following sections, these three models are referred to as the stochastic, robust, and min-max regret models, respectively.

In most papers of literature on BSC network design problems that consider multiple uncertain parameters (Ahmadvand and Sowlati, 2022; Alizadeh et al., 2019; Kumar et al., 2022; Samani and Hosseini-Motlagh, 2021; Zarei et al., 2022) or concurrent uncertainty and disruption (Fattahi and Govindan, 2018; Habib et al., 2022; Mousavi Ahranjani et al., 2020; Salehi et al., 2022), it is commonly assumed that these uncertain parameters are statistically independent. In other words, this assumption asserts that the fluctuation of one parameter does not affect the realization of other uncertain parameters. This assumption is made to simplify the problem-solving process and accommodate various technical considerations. In contrast to prior studies, this research has not considered the assumption of independency among uncertain parameters. This deviation stems from the recognition that, in practice, the quantity of available biomass directly influences its price (Bang et al., 2013). Therefore, the average biomass price in this paper depends on its yield. Furthermore, it is assumed that the biomass price can vary around this average value due to factors such as economic conditions, which is a more realistic assumption. Thus, in the proposed models, the price of biomass is not deterministic after the disruption scenario realization, and it can fluctuate according to its probability distribution.

The main contributions of this study from a modeling perspective are as follows: (1) the integration of uncertainty and disruption into BSC network design problems simultaneously, (2) the development of a stochastic model for the BSC network design problem, (3) the formulation of a robust model with the confidence level, (4) the introduction of the min-max regret model, (5) the assumption of dependency between uncertain parameters, and (6) the consideration of fluctuations in biomass prices around their mean values after the realization of disruption scenarios. From a methodological perspective, an exact algorithm is developed based on the benders decomposition algorithm with an acceleration technique to address the challenges posed by large-scale instances of the problem.

The remainder of this article is organized as follows. Section 2 provides a review of the relevant literature. Section 3 outlines the problem statement. Sections 4 and 5 describe the mathematical formulation of the proposed model and the solution methodology, respectively. Section 6 presents the case study along with the results of the computational experiments. Section 7 offers managerial insights derived from the analysis, emphasizing the practical relevance of the findings for decision-makers. Finally, Section 8 concludes the paper by summarizing the main contributions and proposing directions for future research.

## 2. Literature Review

In this section, the relevant literature on the modeling of BSC networks is reviewed. The literature review has revealed that various mathematical models have been developed for the BSC network, varying in complexity, analysis scope, and level of detail. While some models focus on specific aspects of the supply chain, such as transportation or inventory management, others provide a more comprehensive analysis of the entire BSC network.

### 2.1. Mathematical modeling

Over the past decade, mathematical modeling has played a critical role in optimizing BSCs, progressively evolving from conventional network design problems toward integrated, flexible, and uncertainty-resilient frameworks. One of the earliest integrated models was proposed by Eksiöğlu et al. (2009), who formulated a comprehensive

mixed-integer linear programming (MILP) model for the design of BSC networks. Their work simultaneously optimized facility location, sizing, transportation flows, and inventory management, providing a foundation for subsequent advancements in holistic supply chain design.

Building on this, Paulo et al. (2013) developed an integrated MILP model for biorefinery supply chain design, incorporating multiple biomass types, storage and pre-processing options, transportation alternatives, various processing technologies, and multiple end-product markets. In subsequent work, Paulo et al. (2015) tailored the approach to optimize the supply chain for residual forestry biomass for bioelectricity production in Portugal. Their MILP model simultaneously determined facility locations, production capacities, biomass sourcing strategies, and transportation routes, aiming to minimize total supply chain costs. Recognizing the importance of uncertainty in biomass supply chains, Paulo et al. (2017) introduced a two-stage stochastic MILP model to design integrated BSCs under uncertain biomass availability and technological performance. Scenario reduction techniques were employed to manage computational complexity while maintaining solution robustness.

In parallel, efforts to incorporate sustainability and multi-objective decision-making gained momentum. Petridis et al. (2018) developed a weighted goal programming MILP framework to balance environmental, economic, and social criteria in BSCs. Similarly, Wheeler et al. (2018) combined multi-objective optimization with multi-attribute decision-making methods to facilitate the selection of supply chain configurations aligned with diverse stakeholder preferences. Subsequent advancements focused on enhancing flexibility and adaptability. Allman et al. (2021) proposed an optimization model employing mobile and modular processing units to address spatial and volume uncertainties. Aranguren and Castillo-Villar (2022) introduced a bi-objective two-stage stochastic model for biomass co-firing supply chains, using particle swarm optimization and simulated annealing to explore trade-offs between cost minimization and emission reduction.

Addressing uncertainty, Cao et al. (2021) proposed a tabu search-based heuristic for solving the location-routing problem in BSCs. Recently, Lima et al. (2023) presented a scenario-based MILP model to design the sugar-bioethanol supply chain, maximizing the expected net present value under demand uncertainty. Additionally, Paulo et al. (2023) developed an integrated optimization and discrete-event simulation framework for designing biomass supply chains, focusing on technological learning and the uncertainties associated with biorefinery technologies.

Overall, the evolution of mathematical modeling in BSC design reflects a shift from deterministic, cost-focused strategies to integrated, sustainable, and resilient approaches that effectively manage the inherent challenges in biomass-based industries. Extending this trend, recent studies have increasingly incorporated risk management concepts into BSC modeling, resulting in a range of MILP and mixed-integer non-linear programming models discussed in the following sections.

## 2.2. Uncertainty and disruption modeling approaches

Uncertainty and disruption pose a significant challenge in the long-term decision-making process of the BSC network design problem and can lead to adverse effects on its performance. Compared to conventional fuels, biofuels face a higher level of uncertainty in future biomass supply. Furthermore, the BSC is plagued by other significant uncertainties, including transportation, production, and operational uncertainties, as well as uncertainty in biofuel demand. The supply and price of biomass are uncertain because their production yields are subject to weather disruption, insect populations, plant disease, and farmer planting decisions for the upcoming season (Marufuzzaman et al., 2014). To effectively address these challenges, researchers have employed several methodological approaches. Among them, stochastic programming and robust optimization have emerged as the two principal and most widely applied methods (Ghaderi et al., 2016; Habibi

et al., 2023). Stochastic programming adopts a risk-neutral perspective by incorporating probabilistic information of uncertain parameters to optimize expected outcomes. In contrast, robust models take a risk-averse approach, offering solutions that remain effective across a range of uncertain scenarios without requiring precise probability distributions (Fattahi and Govindan, 2018).

Several notable studies have utilized stochastic approaches in modeling BSC networks, including the works of Cundiff et al. (1997), Dal-Mas et al. (2011), Kim et al. (2011), Chen and Fan (2012), Gonela et al. (2015), and Paulo et al. (2017). In contrast, other researchers, such as Tay et al. (2013), Pishvaei et al. (2012), Shabani and Sowlati (2016), and Bairamzadeh et al. (2016) have extended BSC network formulations by incorporating robust optimization techniques to address uncertainty from a risk-averse perspective.

### 2.2.1. Stochastic programming approaches

To effectively address uncertainties in biomass supply and demand, researchers have proposed various stochastic optimization models. Cundiff et al. (1997) addressed the impact of varying weather scenarios on biomass quality and production by reformulating their model into a two-stage stochastic framework. This allowed them to explicitly incorporate uncertainties in biomass supply. Similarly, Dal-Mas et al. (2011) developed a MILP model aimed at helping decision-makers and investors evaluate BSC investment opportunities under uncertainty in production costs and market prices. Their stochastic formulation incorporated financial performance metrics such as expected net present value and conditional value at risk (CVaR) to capture risk more effectively.

Kim et al. (2011) proposed a two-stage stochastic model for designing a BSC network that accounts for uncertainties in biomass supply, demand, prices, and processing technologies. They treated the selection of biorefinery locations and capacities as first-stage decisions, while operational flows were determined in the second stage across multiple scenarios. In a related effort, Gonela et al. (2015) designed a hybrid-generation bioethanol supply chain that considered sustainability dimensions (i.e., economic, environmental, and social aspect) under uncertainty, using a stochastic MILP approach.

Addressing disruption risks, Poudel et al. (2016) developed a pre-disaster planning model aimed at mitigating failures in transportation infrastructure caused by natural events. Their strategy focused on cost-effective fortification within budget constraints. Maheshwari et al. (2017) also tackled disruption risks, developing a stochastic model to minimize expected costs while accounting for biomass availability fluctuations due to extreme weather events like floods and droughts. Ghelichi et al. (2018) designed a green biodiesel supply chain based on *Jatropha Curcas*, applying a min-max regret approach within a stochastic MILP framework to handle uncertainty in demand and crop yield.

Fattahi and Govindan (2018) took a comprehensive approach to simultaneously address uncertainty and disruption by modeling variability in biomass yield and facility capacity within a multi-stage stochastic framework. Saghaei et al. (2020) introduced a two-stage stochastic mixed-integer non-linear programming model for BSC planning under uncertain climate conditions and market demand. They incorporated a chance constraint to ensure demand satisfaction with 95 % probability, thereby strengthening supply chain resilience. Similarly, Sarkar et al. (2021) focused on disruptions in transportation infrastructure, using a flexible multi-modal transport model and a two-stage stochastic approach with CVaR as the risk measure. Their work highlighted the value of proactive measures such as contract flexibility, infrastructure fortification, alternative routing, and emergency inventory positioning.

Khezerlou et al. (2021) developed a model to design a resilient BSC network considering facility and transportation disruptions. They applied absolute semi-deviation and CVaR to enhance solution resilience. Aranguren and Castillo-Villar (2022) addressed uncertainty in

biomass yield through a multi-objective two-stage stochastic model designed for large-scale BSC planning. Their model aimed to minimize investment costs and environmental impact, treating storage location decisions as first-stage variables. Several other studies, including [Chen et al. \(2012\)](#) and [Memişoğlu et al. \(2021\)](#), have also employed stochastic programming methods to account for uncertainty in various aspects of biofuel industry planning.

### 2.2.2. Robust optimization approach

The robust optimization approach is another widely applied mathematical modeling technique for managing parametric uncertainty in BSCs. [Tay et al. \(2013\)](#) proposed a mixed-integer non-linear programming model that incorporates long-term uncertainties, such as biomass supply and biofuel demand, into the design phase using scenario-based robust optimization techniques. To address multi-objective problems involving uncertain parameters in the objective function, [Bairamzadeh et al. \(2016\)](#) developed a bi-objective robust possibilistic programming approach. Their MILP model optimized a lignocellulosic BSC under uncertainty in biomass market price, biofuel price and demand, and environmental impact coefficients. [Zhang et al. \(2017\)](#) proposed a robust MILP model to design a BSC network at strategic and tactical levels under biodiesel price uncertainty. Their model, based on interval uncertainty, incorporated economic, environmental, and social objectives.

[Razm et al. \(2021\)](#) proposed a two-phase sequential method for BSC network design under uncertainty. The first phase employed multi-criteria decision-making and geographic and social data to determine optimal plant locations. The second phase used a robust optimization model based on [Bertsimas et al. \(2004\)](#) to manage supply chain uncertainty.

[Samani and Hosseini-Motlagh \(2021\)](#) addressed the challenge of sustainable and efficient BSC network design through a multi-period, multi-product model under uncertainty. They applied a mixed robust-possibilistic programming approach to capture parameter uncertainty. Similarly, [Gumte et al. \(2021\)](#) designed a nationwide BSC network using robust optimization and machine learning methods. [Salehi et al. \(2022\)](#) developed a model for a resilient and sustainable BSC network under demand uncertainty and biorefinery disruption. They used a multi-criteria decision-making method to prioritize sustainability indicators and resilience factors, incorporating high-priority elements into their model. A robust-possibilistic programming method was applied to address demand uncertainty in the final formulation.

### 2.2.3. Hybrid methods

To address the complexity and diversity of uncertainties in BSCs, several studies have adopted hybrid modeling approaches that integrate robust and stochastic optimization methods. [Shabani and Sowlati \(2016\)](#) introduced a hybrid stochastic-robust model. They first applied a robust optimization model to address uncertainty in biomass quality, then integrated a stochastic method to capture biomass yield variability.

Recently, [Mousavi Ahranjani et al. \(2020\)](#) proposed a MILP model with a hybrid stochastic-robust-possibilistic programming structure to enhance resilience against fluctuations in biomass supply, demand, and pricing. [Alizadeh et al. \(2019\)](#) designed a reliable and cost-effective BSC network using a hybrid robust-stochastic approach. They modeled biomass seasonality and carbon tax rate uncertainties through probabilistic scenarios and uncertainty sets. A three-stage stochastic model was developed by integrating an adjustable robust method with the sample average approximation scheme.

Recent studies in BSC modeling have increasingly adopted hybrid uncertainty approaches to enhance model robustness and realism. These methods are particularly useful when multiple uncertain parameters exist, each characterized by different levels of information availability. When the probability distributions of all uncertain parameters are known, stochastic programming serves as a suitable method for capturing uncertainty ([Dal-Mas et al., 2011](#); [Gonela et al., 2015](#); [Kim](#)

[et al., 2011](#)). However, in many practical situations, only partial distributional information is available. In such cases, hybrid frameworks, such as stochastic-robust, robust-stochastic, or stochastic-adaptive-robust models, have been effectively employed to address heterogeneous uncertainty ([Alizadeh et al., 2019](#); [Mousavi Ahranjani et al., 2020](#); [Shabani and Sowlati, 2016](#)).

Despite these advancements, a critical shortcoming in most existing models is the assumption of independence among uncertain parameters. This simplification fails to capture the inherent dependencies between key variables. For instance, biomass price is often contingent upon its regional availability, and market demand for biofuels typically fluctuates with fuel pricing. Ignoring such dependencies can lead to biased estimates and suboptimal decisions in network design and planning.

To address this gap, this study introduces a two-layer uncertainty modeling structure, where second-layer parameters are conditionally dependent on the realization of first-layer parameters. Based on the nature and availability of distributional information, uncertainty approaches can be classified into three categories:

1. Type I: when both layers have known probability distributions, stochastic programming and robust technique (with discrete scenario) are applicable ([Dal-Mas et al., 2011](#); [Gonela et al., 2015](#); [Kim et al., 2011](#)).
2. Type II: when only first-layer parameters have known distributions, hybrid methods such as stochastic-robust and stochastic-adaptive-robust are suitable ([Mousavi Ahranjani et al., 2020](#); [Shabani and Sowlati, 2016](#)).
3. Type III: when only second-layer parameters are specified with known distributions, min-max regret, robust-stochastic, and adaptive-robust-stochastic models are more appropriate ([Chen et al., 2020](#); [Taherkhani et al., 2021](#)), depending on whether the first-layer scenarios are discrete or continuous.

By explicitly capturing the interdependencies among uncertain parameters, the proposed framework advances the current state of BSC modeling and facilitates more adaptive and informed decision-making under uncertainty. This study considers two distinct uncertainty settings: (i) when full distributional information is available for both layers (Type I), addressed through the development of stochastic ([Gonela et al., 2015](#); [Taherkhani et al., 2021](#)) and robust ([Peykani et al., 2020](#)) models; and (ii) when the first-layer distributions are unknown and the second-layer distributions are known (Type III), addressed through the formulation of a min-max regret model ([Taherkhani et al., 2021](#)). This comprehensive treatment improves the model's applicability in the presence of disruption and limited information.

The difference between the BSC network design model presented in this paper and the literature referenced are outlined in [Table 1](#). In this table, the abbreviations DP, SP, and RO denote dependency between parameters, stochastic programming, and robust optimization, respectively. The biomass availability and biomass quality parameter are denoted by BA and BQ in [Table 1](#), respectively. Supply chain operational costs, including transportation costs and production costs, are abbreviated as OC. Meanwhile, D, PC, BD, and TC represent biofuel demand, biomass price, benders decomposition, and technology and capacity of facility, respectively.

## 3. Problem description

This paper aims to determine the BSC network under both uncertainty and disruption. The BSC network comprises several levels, including biomass suppliers (farms), biofuel production plants (biorefineries), distributors (biofuel storage facilities), and consumers (cities), as depicted in [Fig. 1](#).

A multi-period planning horizon is considered to capture the temporal structure of the supply chain decisions. All biomass required for biofuel production is purchased at the beginning of the planning horizon



**Table 1**  
Literature review.

Paper	BSC risk		Modeling method		DP	BD algorithm	Uncertain parameter					
	Uncertainty	Disruption	SP	RO			BA	BQ	OC	D	PC	TC
Dal-Mas et al. (2011)	*		*						*		*	
Kim et al. (2011)	*		*				*			*	*	
Chen and Fan (2012)	*		*				*				*	
Tay et al. (2013)	*			*			*			*		
Gonela et al. (2015)	*		*				*			*	*	
Bairamzadeh et al. (2016)	*			*			*					
Shabani and Sowlati (2016)	*			*			*	*				
Poudel et al. (2016)		*	*			*						*
Zhang and Jiang (2017)	*			*							*	
Paulo et al. (2017)	*		*				*					*
Maheshwari et al. (2017)		*	*				*					
Ghelichi et al. (2018)	*		*				*			*		
Fattahi and Govindan (2018)	*	*	*				*					*
Alizadeh et al. (2019)	*			*			*					
Mousavi Ahranjani et al. (2020)	*	*	*				*		*			
Saghaei et al. (2020)		*	*				*					
Razm et al. (2021)	*			*			*					
Khezerlou et al. (2021)			*									*
Memişoğlu and Üster (2021)	*		*			*	*					
Sarkar et al. (2021)		*		*								*
Allman et al. (2021)	*		*				*					
Aranguren and Castillo-Villar (2022)	*		*				*	*				
Salehi et al. (2022)	*	*		*								*
Lima et al. (2023)	*		*							*		
Paulo et al. (2023)	*		*									*
This paper	*	*	*	*	*	*	*		*			

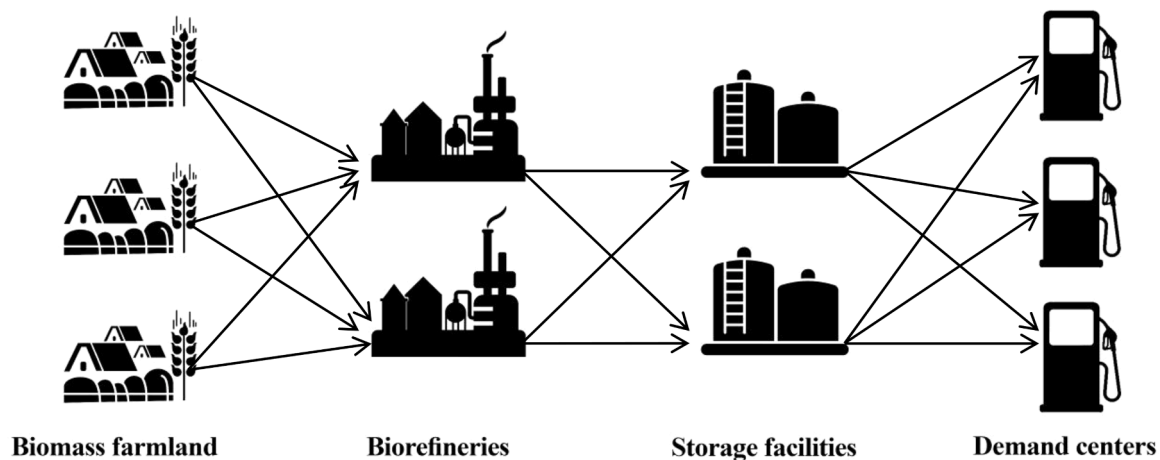


**Fig. 1.** Proposed biofuel supply chain structure.

from farms with known locations, and is subsequently transported to biorefineries. In each period, the transported biomass undergoes a specific process involving pre-treatment, fermentation, distillation, and solid recycling to produce biofuel. The resulting biofuel is then sent to the distributor's storage facilities and then distributed to consumers. In the cases which customer demand exceeds the available biofuel supply amount, the necessary quantity of biofuel must be imported to meet the demand.

Natural phenomena such as floods, storms, and severe climate changes have a detrimental effect on biomass yield. As a result, biomass availability in a particular region may not meet the anticipated volumes. This shortage of biomass imposes limitations on the production of biofuels. Therefore, to make the problem more realistic, it is assumed that biomass availability can be disrupted and decrease significantly. Additionally, the purchase price of biomass is considered to be uncertain.

This study accounts for the dependency between biomass availability and its market price, recognizing that reduced supply typically leads to higher prices (Bang et al., 2013). To reflect this dependency, biomass

price is modeled as a linear function of its availability, a common approach in economic modeling (Mankiw, 2021). To enhance realism and account for market complexities beyond the linear assumption, an uncertainty term is incorporated, which is introduced in this study as an error function. This error function reflects the impact of various external factors, such as demand fluctuations, competition from alternative products, and broader market dynamics, which can influence biomass pricing.

Disruption events typically lead to a reduction in the available biomass, which in turn causes a leftward shift in the supply curve (Mankiw, 2021). This shift reflects a decrease in biomass availability, which in turn leads to higher market prices. Fig. 2 illustrates this effect, showing how supply-side disruptions contribute to price increases by decreasing biomass availability. Fig. 2 also shows the effect of the error function at the equilibrium point of supply and demand, demonstrating the influence of additional market factors that affect biomass pricing.

To design a resilient BSC network, nine decision types are considered: (1) location decisions, (2) capacity decisions, (3) technology

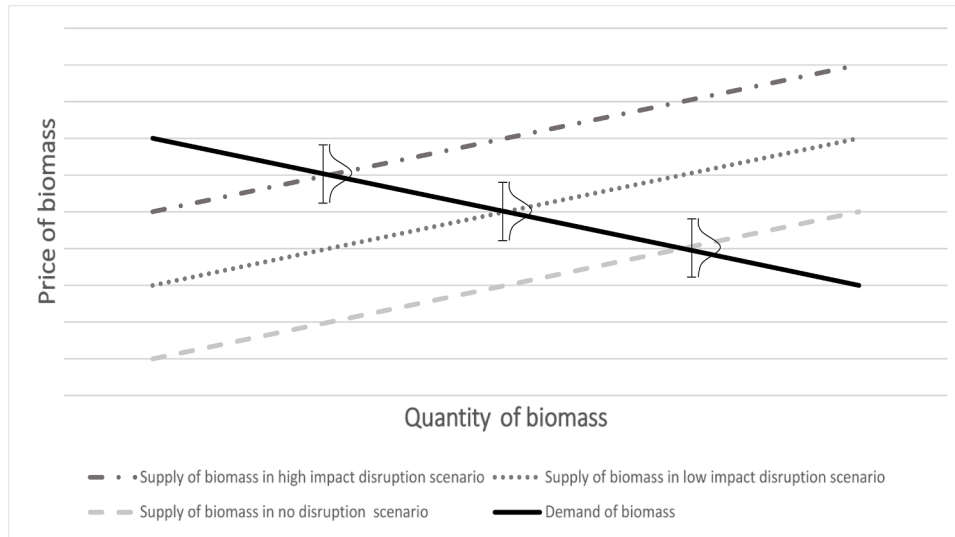


Fig. 2. supply-demand diagram of biomass.

decisions, (4) biomass procurement decisions, (5) production decisions, (6) transportation decisions, (7) biofuel importation decisions, (8) inventory decisions, and (9) distribution decisions. Facility locations, nominal capacities, and biorefinery technologies as strategic decisions are made at the beginning of the planning horizon, before the realization of uncertainty and disruption scenarios. These decisions remain fixed during the planning horizon.

After the strategic decisions are made, the impact of potential disruptions on biomass availability becomes apparent at the beginning of the planning horizon. This step clarifies the actual quantity of biomass accessible from each supplier. Subsequently, the uncertainty regarding biomass purchase prices is realized. Based on these revealed conditions, procurement decisions are made. Thereafter, during each time period, tactical decisions are executed, including transportation decisions, biofuel import decisions, inventory decisions, and distribution decisions, along with biomass allocation to biorefineries and scheduling of

production processes (Fig. 3).

The decision-making steps in this problem can be summarized as follows: Initially, strategic decisions are made. Subsequently, disruption scenarios are realized, which determine the availability of biomass. Following that, biomass price scenarios are realized then the purchase price of biomass is determined. It is important to note that the availability and prices remain constant for all periods in the planning horizon. Finally, based on all the preceding information, tactical decisions are made. These steps are illustrated in

#### 4. Model formulation

To formulate the mathematical models of the introduced problem, initially, the notations for sets, parameters, and decision variables are defined. Subsequently, the mathematical models are presented.

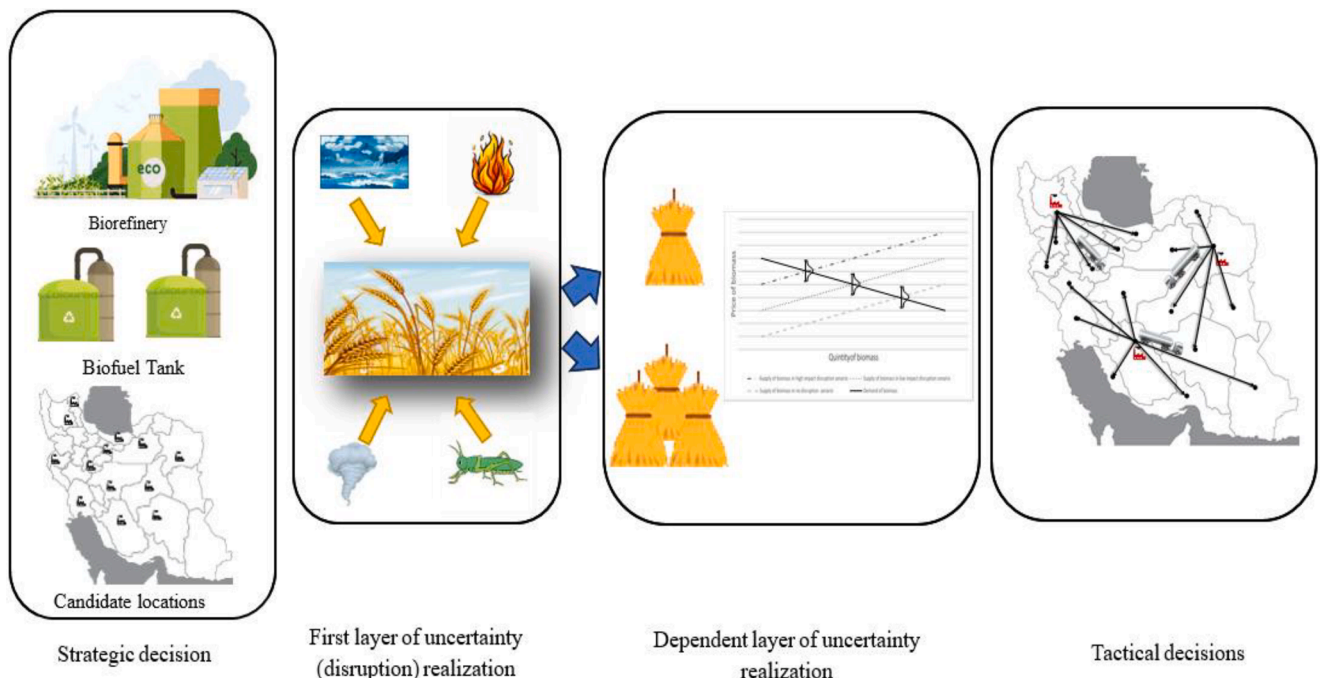


Fig. 3. The decision-making steps.

#### 4.1. Notations

Notations used for the mathematical formulation of the proposed models are demonstrated in Table 2 as follows.

#### 4.2. Dependency of uncertain parameters

In the proposed problem, the biomass procurement price is considered linearly depend on the biomass availability realization. More specifically, let  $\beta'_l$  denote the expected yield of biomass before the occurrence of a disruption, while for biomass type,  $\beta''_{ls}$  represents the available amount of biomass following the realization of disruption scenario  $s$ . Additionally,  $\varphi'_{ls}$  demonstrates the mean value of biomass price and  $\widehat{\varphi}_l$  denotes its nominal value. Dependence of  $\varphi'_{ls}$  to  $\beta''_{ls}$  for a given disruption scenario is shown as follows:

$$\varphi'_{ls} = \widehat{\varphi}_l + \psi(\beta'_l - \beta''_{ls}) \forall l, s \quad (1)$$

where  $\psi$  is assumed to be a positive coefficient that represents the dependency of the biomass price on its availability. Eq. (1) indicates the linear dependency between the mean value of biomass price and the biomass availability realization. This equation states that a decrease in the biomass availability after disruption leads to an increase in the mean biomass price value. Additionally, the realization of the biomass price is assumed to fluctuate around its mean value, independent of disruption effects, which are denoted by price error function  $\varepsilon_l(\xi_s)$ . Therefore, Eq. (2) can be utilized to calculate the biomass price  $\varphi_l(\xi_s)$  as follows:

$$\varphi_l(\xi_s) = \varphi'_{ls} + \varepsilon_l(\xi_s) \forall l, s, \xi_s \quad (2)$$

As depicted in Fig. 2, the mean value of biomass price is linearly dependent on the biomass availability realization, and the biomass price realization fluctuates around its mean value.

#### 4.3. Stochastic model

In this section, it is assumed that sufficient historical data is available to estimate the probability distribution of uncertainties and disruptions. Based on this estimation, the mathematical model of the problem is developed. The proposed model captures biomass procurement costs and availability under a finite set of scenarios. The objective function of the stochastic model is formulated to minimize the expected total cost.

$$\min TF + TE + \mathbb{E}_{\xi_s} [SC(\xi_s) + PC(\xi_s) + BC(\xi_s) + IC(\xi_s) + RC(\xi_s)] \quad (3)$$

s.to:

$$TF = \sum_j \sum_n \sum_q \delta_{jnq} z_{jnq} \quad (4)$$

$$TE = \sum_k \sum_n \sigma_{kn} w_{kn} \quad (5)$$

$$SC(\xi_s) = \sum_j \sum_k \sum_t \tau_{jkt} y_{jkt}(\xi_s) + \sum_k \sum_m \sum_t \tau_{kmt} v_{kmt}(\xi_s) + \sum_o \sum_m \sum_t \tau_{omt} e_{omt}(\xi_s) + \sum_i \sum_l \sum_j \lambda_{ijl} x_{ijl}(\xi_s) \forall s, \xi_s \quad (6)$$

$$PC(\xi_s) = \sum_j \sum_q \gamma_{jq} p_{jq}(\xi_s) \forall s, \xi_s \quad (7)$$

$$BC(\xi_s) = \sum_l \sum_i \varphi_l(\xi_s) h_{il}(\xi_s) \forall s, \xi_s \quad (8)$$

$$IC(\xi_s) = \sum_o \sum_m \sum_t \alpha e_{omt}(\xi_s) \forall s, \xi_s \quad (9)$$

$$RC(\xi_s) = \sum_k \sum_t \nu b_{kt}(\xi_s) \forall s, \xi_s \quad (10)$$

**Table 2**

Sets, parameters, and variable notations.

Sets :	
$l \in L$	Set of biomass type
$i \in I$	Set of farmlands (i.e., biomass harvesting location)
$j \in J$	Set of biorefinery candidate locations
$k \in K$	Set of biofuel storage candidate locations
$o \in O$	Set of candidate ports for importing biofuel
$t \in T$	Set of time periods
$n \in N$	Set of capacity levels (small, medium, and large) for biorefineries and biofuel storage facilities
$q \in Q$	Set of biorefinery technologies type
$m \in M$	Set of customers
$s \in S$	Set of biomass disruption scenarios
$\xi_s \in \Xi_s$	Set of biomass price scenarios under disruption scenario $s$
Parameters :	
$\beta_{il}$	The yield of biomass type $l$ (ton) in farmland $i$ before disruption
$\rho_{is}$	The percentage of biomass unaffected by the disruption in farmland $i$ in disruption scenario $s$
$\beta'_l$	Total yield of biomass type $l$ (ton) before disruption scenarios are realized ( $\beta'_l = \sum_i \beta_{il}$ )
$\beta''_{ls}$	Total yield of biomass type $l$ (ton) after realization of disruption scenario $s$ ( $\beta''_{ls} = \sum_i \beta_{il} \rho_{is}$ )
$\gamma$	The unit production cost (\$/gallon) of biofuel
$\varphi_l(\xi_s)$	The unit procurement cost (\$/ton) of biomass type $l$ in scenario $\xi_s$
$\varphi'_{ls}$	The mean value of procurement cost (\$/ton) of biomass type $l$ in scenario $s$
$\widehat{\varphi}_l$	The nominal procurement cost (\$/ton) of biomass type $l$
$\pi_{jnq}$	The maximum allowed capacity (gallon) for biorefinery in location $j$ with capacity level $n$ and technology type $q$
$\mu_{kn}$	Biofuel storage capacity (gallon) in location $k$ with capacity level $n$
$\tau_{jk}$	The unit transportation cost for biofuel (\$/gallon) between node $j$ ( $\in j, k$ ) and $k$ ( $\in k, m$ )
$\nu$	The unit inventory cost for biofuel (\$/gallon)
$\lambda_{ijl}$	The unit transportation cost for biomass type $l$ (\$/ton) between node $i$ and $j$
$\theta_{mt}$	Biofuel demand of customer $m$ (gallon) in time period $t$
$\delta_{jnq}$	The investment cost (\$) for establishing biorefinery in the location $j$ with capacity level $n$ and technology type $q$
$\sigma_{kn}$	The investment cost (\$) for establishing biofuel storage in the location $k$ with capacity level $n$
$\alpha$	The unit importation cost (\$/gallon) of biofuel
$\varepsilon_l(\xi_s)$	Price error function for biomass type $l$ in scenario $\xi_s$
$\kappa$	Confidence level
$\chi$	The upper bound of BSC cost
$\zeta(\xi_s)$	Probability of scenario $\xi_s$
$\eta_{lq}$	Conversion rate of biomass type $l$ into biofuel with technology type $q$
$\psi$	A positive coefficient that represents the dependency of the biomass price on its availability
Variables:	
$z_{jnq}$	A binary variable that is 1 if biorefinery is established in the location $j$ with capacity level $n$ and technology type $q$
$w_{kn}$	A binary variable that is 1 if biofuel storage is established in the location $k$ with capacity level $n$
$x_{ijl}(\xi_s)$	A non-negative variable representing the amount of transported biomass type $l$ (ton) from farmland in location $i$ into established biorefinery in location $j$ in scenario $\xi_s$
$y_{jkt}(\xi_s)$	A non-negative variable representing the amount of transported biofuel (gallon) from established biorefinery in location $j$ into established biofuel storage facility in location $k$ in time period $t$ in scenario $\xi_s$
$v_{kmt}(\xi_s)$	A non-negative variable representing the amount of transported biofuel (gallon) from established biofuel storage in location $k$ into the customer $m$ in time period $t$ in scenario $\xi_s$
$e_{omt}(\xi_s)$	A non-negative variable representing the amount of imported biofuel (gallon) from port $o$ to satisfy the demand of customer $m$ in time period $t$ in scenario $\xi_s$
$h_{il}(\xi_s)$	A non-negative variable representing the amount of purchased biomass (ton) of type $l$ from farmland $i$ in scenario $\xi_s$
$p_{jq}(\xi_s)$	A non-negative variable representing the amount of produced biofuel (gallon) in established biorefinery in location $j$ with technology type $q$ in time period $t$ in scenario $\xi_s$
$b_{kt}(\xi_s)$	Inventory level of established biofuel storage facility in location $k$ at the end of time period $t$ in scenario $\xi_s$
$a(\xi_s)$	A binary variable that is 1 if BSC cost being less than or equal to target threshold
$TF$	Total investment cost of establishing biorefineries
$TE$	Total investment cost of establishing storage facilities
$SC(\xi_s)$	Total shipping cost in scenario $\xi_s$

(continued on next page)

Table 2 (continued)

Sets :	
$PC(\xi_s)$	Total production cost in scenario $\xi_s$
$BC(\xi_s)$	Total purchasing cost of biomass in scenario $\xi_s$
$IC(\xi_s)$	Total importing cost of biofuel in scenario $\xi_s$
$RC(\xi_s)$	Total inventory cost of biofuel in scenario $\xi_s$

The investment costs associated with establishing biorefineries and storage facilities are represented by the first and second terms of the objective function in Eq. (3), respectively. These terms reflect the fixed capital investment costs required for infrastructure development at selected locations, capacity levels, and production technologies. Moreover, the third to seventh terms in Eq. (3) account for the expected operational costs under uncertainty, including transportation of biomass and biofuel, biofuel production, biomass procurement, and biofuel importation. These components collectively define the total expected cost that the model seeks to minimize. The investment costs related to establishing biorefineries and constructing biofuel storage facilities are formulated in Eq. (4) and Eq. (5), respectively. Eq. (6) represents the total transportation cost, encompassing biomass transportation from farmlands to biorefineries, biofuel shipment from production plants to storage facilities, and subsequent distribution from storage sites and ports to end customers. The cost of biofuel production is modeled in Eq. (7). Eq. (8) estimates biomass procurement costs, while Eqs. (9) and (10) jointly account for the cost associated with biofuel imports and the storage of biofuels at designated facilities, respectively.

$$\sum_i \sum_l \eta_{ilq} x_{ilj}(\xi_s) = \sum_t p_{jqt}(\xi_s) \forall j, q, s, \xi_s \quad (11)$$

$$\sum_q p_{jqt}(\xi_s) = \sum_k y_{jkt}(\xi_s) \forall j, t, s, \xi_s \quad (12)$$

$$p_{jqt}(\xi_s) \leq \sum_n \pi_{jnq} z_{jnq} \forall j, q, t, s, \xi_s \quad (13)$$

$$\sum_n \sum_q z_{jnq} \leq 1 \forall j \quad (14)$$

Eq. (11) ensures the mass balance between the amount of biomass transported to biorefinery  $j$  with technology  $q$  and the corresponding quantity of biofuel produced. Specifically, the total amount of biomass of type  $l$  delivered from all farmland locations  $i$ , multiplied by the biomass-to-biofuel conversion rate  $\eta_{ilq}$ , must be equal to the biorefinery's total output. This constraint guarantees that the production level is consistent with the availability of different biomass types and the efficiency of the selected production technology. Eq. (12) guarantees that the total amount of biofuel produced in each biorefinery is entirely transported to designated storage facilities. This constraint ensures no accumulation or loss of biofuel at the production site, thereby maintaining flow continuity within the supply chain network. Eqs. (13) and (14) jointly represent the technical and structural limitations related to biofuel production. Eq. (13) ensures that the production level at each active biorefinery does not exceed its designated nominal capacity, reflecting the technological limits of the selected facility. Moreover, Eq. (14) imposes a location-specific restriction by assuming that only one biorefinery, with a specific technology and capacity level, can be established in each candidate region.

$$h_{il}(\xi_s) \leq \beta_{il} \rho_{is} \forall i, l, s, \xi_s \quad (15)$$

$$h_{il}(\xi_s) = \sum_j x_{ilj}(\xi_s) \forall i, l, s, \xi_s \quad (16)$$

Eq. (15) ensures that the entire quantity of biomass intended for use is purchased at the beginning of the planning horizon. Moreover, the amount procured from each harvesting region must not exceed the locally available biomass yield. Eq. (16) guarantees that the total

amount of biomass transported to biorefineries is equal to the total biomass purchased at the beginning of the planning period. This ensures mass balance and prevents any discrepancy between procurement and utilization.

$$b_{kt}(\xi_s) = b_{k,(t-1)}(\xi_s) + \sum_j y_{jkt}(\xi_s) - \sum_m v_{kmt}(\xi_s) \forall k, t, s, \xi_s, t \neq 1 \quad (17)$$

$$b_{kt}(\xi_s) = \sum_j y_{jkt}(\xi_s) - \sum_m v_{kmt}(\xi_s) \forall k, t, s, \xi_s, t = 1 \quad (18)$$

$$b_{kt}(\xi_s) \leq \sum_n \mu_{kn} w_{kn} \forall k, t, s, \xi_s \quad (19)$$

$$\sum_n w_{kn} \leq 1 \forall k \quad (20)$$

Eq. (17) models the inventory balance at each storage facility for all periods except the initial one. It states that the inventory level at each time period equals the inventory at the end of the previous period, plus the amount of biofuel received from biorefineries, minus the amount dispatched to customers. This constraint ensures temporal consistency in inventory tracking throughout the planning horizon. Eq. (18) defines the inventory level for the first period. It assumes that the initial inventory at the beginning of the planning horizon is zero, thereby initializing the flow of biofuel in the system. Eq. (19) ensures that the inventory level at the end of each time period in any active storage facility does not exceed its designated storage capacity. Eq. (20) ensures that at most one storage facility with a specific capacity level can be established at each candidate location. This constraint enforces the exclusivity of storage investment decisions and prevents the simultaneous construction of multiple facilities at the same site.

$$\sum_k v_{kmt}(\xi_s) + \sum_o e_{omt}(\xi_s) = \theta_{mt} \forall m, t, s, \xi_s \quad (21)$$

$$x_{iljt}(\xi_s), y_{jkt}(\xi_s), v_{kmt}(\xi_s), e_{omt}(\xi_s), h_{il}(\xi_s), p_{jqt}(\xi_s) \in \mathbb{R}_+ \forall i, j, l, k, m, q, t, s, \xi_s \quad (22)$$

$$z_{jnq}, w_{kn} \in \{0, 1\} \forall j, n, q, s, k \quad (23)$$

Eq. (21) ensures that, in each time period, the entire biofuel demand of every customer is satisfied either through production or importation. This constraint maintains demand fulfillment across the planning horizon and guarantees supply adequacy. Eq. (22) and Eq. (23) define the domain of non-negative continuous variables and binary decision variables, which represent flows, production levels, inventories, and discrete choices in the model.

#### 4.4. Robust model

A key characteristic of disruption risk is its significant impact on the supply chain structure despite its low probability of occurrence. Incorporating high-impact, low-probability scenarios into the modeling process can significantly alter the configuration and total costs of the supply chain. However, some decision-makers prefer to focus only on scenarios with a higher probability, modeling the problem to ensure feasibility for the more probable scenarios while excluding scare scenarios. To address this preference, this study introduces the robust model designed to minimize the target threshold of the total BSC cost ( $B$ ) while explicitly considering a predefined confidence level ( $\kappa$ ). In other words, this model designs a BSC network, which minimizes  $B$  while ensuring that the probability of the BSC total cost being less than or equal to  $B$  is at least  $\kappa$ . This approach balances the need for resilience against disruptions with practical considerations of feasibility and cost-effectiveness.

Similar to the stochastic model, the robust model assumes sufficient historical data is available to estimate the probability distribution of uncertain parameters. Consequently, the biomass price and availability are represented by a predefined set of scenarios.



$$\min B \quad (24)$$

s.to:

$$B - (TF + TE + SC(\xi_s) + PC(\xi_s) + BC(\xi_s) + IC(\xi_s) + RC(\xi_s)) \geq \chi(a(\xi_s) - 1) \forall s, \xi_s \quad (25)$$

$$\sum_{\xi_s} \sum_s \zeta(\xi_s) a(\xi_s) \geq \kappa \quad (26)$$

The remaining constraints of the model are given by Eqs. (4)–(23). Eq. (25) states that  $a(\xi_s)$  equals 1 if the BSC cost in the scenario  $\xi_s$  does not exceed  $B$ ; otherwise, it is set to 0. Additionally, Eq. (26) specified that the cumulative probability of scenarios satisfying Eq. (25) must be greater than or equal to the specified confidence level  $\kappa$ .

#### 4.5. Min-max regret model

Given the low probability of specific natural disruptions, historical data is often insufficient to predict the probability distribution of such events accurately. In these situations, supply chain design decisions can benefit from models that do not depend on historical data or predefined probability distributions for disruptions. To address this limitation, this study proposes the min-max regret model. This criterion makes a decision based on the regret of not selecting the best solution. The min-max criterion offers a less conservative approach compared to the worst-case robust model. Consequently, the selection of the most conservative and costly solution is avoided. In this model, a discrete set of disruption scenarios is considered to make robust decisions based on the min-max regret criterion, while the uncertain parameter is still formulated using a stochastic approach. Due to the inherent capability of this method to describe disruption using a finite set of scenarios, it enables the utilization of decomposition solution methods, effectively mitigating the problem-solving burden.

Let  $F^s$  to be the optimal BSC cost for a given realized disruption scenario  $s$ , and let  $F^s(Z)$  to be the total BSC cost for a given solution  $Z$ , which  $Z$  represents strategic decision for simplicity. The maximum regret is obtained by a disruption scenario that maximizes  $F^s(Z) - F^s$ . The goal of the min-max regret criterion, which is employed to formulate the min-max model, is to find  $Z$  that minimize regret function as represented in Eq. (27):

$$\min_Z \max_s [F^s(Z) - F^s] \quad (27)$$

To linearize Eq. (27), the maximum regret function is replaced with a positive variable  $U$ . The decision-making process in this model begins with making strategic decisions. Once the strategic decisions are determined, disruption scenarios  $s$  and their corresponding parameter  $\rho_{is}$  are realized. This is followed by the realization of the biomass price scenario  $\xi_s$ , which depends on the realization of the disruption scenario  $s$ . Finally, tactical decisions are made under both disruption and uncertainty scenarios. Consequently, the min-max regret model, subject to Eqs. (4)–(23), is formulated as follows:

$$\min U \quad (28)$$

s.to:

$$U \geq TF + TE + \mathbb{E}_{\xi_s} [SC(\xi_s) + PC(\xi_s) + BC(\xi_s) + IC(\xi_s) + RC(\xi_s)] - F^s \forall s \quad (29)$$

The following section developed solution methods based on the benders decomposition algorithm for efficiently solving the mathematical models presented in this section.

## 5. Solution algorithms

The proposed models for the BSC network design problem are classified as NP-hard (Dupačová et al., 2003). While commercial solvers like CPLEX are effective for certain problem sizes, the complexity of these models may limit their performance due to the large-scale problems. To effectively solve the proposed models with a large problem size within a reasonable timeframe, an exact solution algorithm that incorporates Benders Decomposition (BD) is presented in this section.

### 5.1. Solution algorithm for stochastic model

This paper develops the BD algorithm to solve the proposed models. The BD algorithm decomposes the main problem into a primal subproblem (PS) and a master problem (MP), reducing the problem's complexity. The BD creates the PS model by fixing the integer variables and then solves the dual subproblem (DS) to obtain information that updates the MP. The PS of the stochastic model, include Eqs. (3)–(23), for fixed first-stage variable can be formulated as:

$$\min \mathbb{E}_{\xi_s} [SC(\xi_s) + PC(\xi_s) + BC(\xi_s) + IC(\xi_s) + RC(\xi_s)] \quad (30)$$

s.to:

$$\sum_i \sum_l \eta_{il} x_{ilj}(\xi_s) = \sum_t p_{jqt}(\xi_s) \forall j, q, s, \xi_s \quad (31)$$

$$\sum_q p_{jqt}(\xi_s) = \sum_k y_{jkt}(\xi_s) \forall j, t, s, \xi_s \quad (32)$$

$$p_{jqt}(\xi_s) \leq \sum_n \pi_{jnq} \bar{z}_{jnq} \forall j, q, t, s, \xi_s \quad (33)$$

$$h_{il}(\xi_s) \leq \beta_{il} \rho_{is} \forall i, l, s, \xi_s \quad (34)$$

$$h_{il}(\xi_s) = \sum_j x_{ilj}(\xi_s) \forall i, l, s, \xi_s \quad (35)$$

$$b_{kt}(\xi_s) = b_{k,(t-1)}(\xi_s) + \sum_j y_{jkt}(\xi_s) - \sum_m v_{kmt}(\xi_s) \forall k, t, s, \xi_s, t \neq 1 \quad (36)$$

$$b_{kt}(\xi_s) = \sum_j y_{jkt}(\xi_s) - \sum_m v_{kmt}(\xi_s) \forall k, t, s, \xi_s, t = 1 \quad (37)$$

$$b_{kt}(\xi_s) \leq \sum_n \mu_{kn} \bar{w}_{kn} \forall k, t, s, \xi_s \quad (38)$$

$$\sum_k v_{kmt}(\xi_s) + \sum_o e_{omt}(\xi_s) = \theta_{mt} \forall m, t, s, \xi_s \quad (39)$$

$$x_{iljt}(\xi_s), y_{jkt}(\xi_s), v_{kmt}(\xi_s), e_{omt}(\xi_s), h_{il}(\xi_s), p_{jqt}(\xi_s) \in \mathbb{R}_+ \forall i, j, l, k, m, q, t, s, \xi_s \quad (40)$$

The values of  $\bar{z}_{jnq}$  and  $\bar{w}_{kn}$  are fixed value of  $z_{jnq}$  and  $w_{kn}$ , respectively, and should be derived from the MP. The BD cut can be computed by solving the DS of the model represented by Eqs. (30)–(40), as outlined below. In Eq. (41),  $u_{jqt\xi_s}$ ,  $t_{il\xi_s}$ ,  $c_{kt\xi_s}$ , and  $g_{mt\xi_s}$  denote the dual variables corresponding to Eqs. (33), (34), (38) and (39) respectively.

$$\omega \geq \sum_s \sum_{\xi_s} \sum_t \left( \sum_m \theta_m \bar{g}_{mt\xi_s} - \sum_j \sum_n \sum_q \pi_{jnq} \bar{z}_{jnq} \bar{u}_{jqt\xi_s} - \sum_i \sum_l \beta_{il} \rho_{is} \bar{t}_{il\xi_s} - \sum_k \sum_n \mu_{kn} \bar{w}_{kn} \bar{c}_{kt\xi_s} \right) \quad (41)$$

The BD optimality cuts are incorporated into the MP by leveraging

the outcomes derived from solving the DS problems. It is noteworthy that the DS problems are always feasible and bounded.

$$\min \sum_j \sum_n \sum_q \delta_{jnq} z_{jnq} + \sum_k \sum_n \sigma_{kn} w_{kn} + \omega \quad (42)$$

s.to:

$$\omega \geq \sum_s \sum_{\xi_s} \sum_t \left( \sum_m \theta_m \bar{g}_{mt\xi_s} - \sum_j \sum_n \sum_q \pi_{jnq} z_{jnq} \bar{u}_{jq t \xi_s} - \sum_i \sum_l \beta_{il} \rho_{is} \bar{t}_{il \xi_s} - \sum_k \sum_n \mu_{kn} w_{kn} \bar{c}_{kt \xi_s} \right) \quad (43)$$

$$\sum_n \sum_q z_{jnq} \leq 1 \quad \forall j \quad (44)$$

$$\sum_n w_{kn} \leq 1 \quad \forall k \quad (45)$$

$$z_{jnq}, w_{kn} \in \{0, 1\} \quad \forall j, k, q, n \quad (46)$$

The BD fixes the solutions derived from the MP in the DS problems and subsequently appends optimality cuts to the MP based on the optimal values obtained from solving the DS problems. This iterative process continues until the difference between the upper and lower bounds on the solution value of the problem becomes acceptably small. Algorithm 1 presents a pseudo-code for the BD algorithm, in which the optimal values of the MP and the DS at iteration  $r$ , denoted as  $F_{MP}^r$  and  $F_{DS}^r$ , respectively, are used to update the algorithm bounds. The upper and lower bounds of the solution value are represented by the  $UB$  and  $LB$ , respectively, and  $P$  denote the set of extreme point of DS. In each iteration of Algorithm 1, the  $UB$  for the stochastic model is computed using the Eq. (47).

$$UB = \sum_j \sum_n \sum_q \delta_{jnq} z_{jnq} + \sum_k \sum_n \sigma_{kn} w_{kn} + F_{DS}^r \quad (47)$$

## 5.2. Solution algorithm for robust model

This section presents the methodology developed to address the robust model using BD algorithm. The PS of the robust model is formulated for fixed values of  $z_{jnq}, w_{kn}$ , and  $a(\xi_s)$ .

$$\min B \quad (48)$$

s.to:

$$B - (TF + TE + SC(\xi_s) + PC(\xi_s) + BC(\xi_s) + IC(\xi_s) + RC(\xi_s)) \geq \chi(\bar{a}(\xi_s) - 1) \quad \forall s, \xi_s \quad (49)$$

Eqs. (31)–(40) represent the remaining constraints that complete the formulation of the model. By redefining  $u_{jq t \xi_s}$ ,  $t_{il \xi_s}$ ,  $c_{kt \xi_s}$ , and  $g_{mt \xi_s}$  as the

### Algorithm 1

Pseudocode of algorithm BD for proposed models.

Benders decomposition algorithm for proposed models
1 : $UB \leftarrow +\infty, LB \leftarrow -\infty, r \leftarrow 1$
2 : $P \leftarrow \emptyset$
3 : <b>while</b> $UB > LB$ <b>do</b>
4 : <b>solve</b> MP of model to obtain $\bar{z}_{MP}^r$ and $\bar{w}_{MP}^r$
5 : $LB \leftarrow F_{MP}^r$
6 : <b>solve</b> DS( $\bar{z}_{MP}^r$ and $\bar{w}_{MP}^r$ ) of model to obtain $u_{jq t \xi_s}$ , $t_{il \xi_s}$ , $c_{kt \xi_s}$ , $g_{mt \xi_s}$ , and $F_{DS}^r$
7 : $P \leftarrow P \cup \left\{ (u_{jq t \xi_s}, t_{il \xi_s}, c_{kt \xi_s}, g_{mt \xi_s})_r \right\}$
8 : <b>update</b> $UB$
9 : $r \leftarrow r + 1$
10 : <b>end while</b>

dual variables associated with the Eqs. (33),(34),(38) and (39) respectively, the corresponding BD cut for the robust model is derived as follows:

$$\omega'(\xi_s) \geq \sum_t \left( \sum_m \theta_m \bar{g}_{mt \xi_s} - \sum_j \sum_n \sum_q \pi_{jnq} z_{jnq} \bar{u}_{jq t \xi_s} - \sum_i \sum_l \beta_{il} \rho_{is} \bar{t}_{il \xi_s} - \sum_k \sum_n \mu_{kn} w_{kn} \bar{c}_{kt \xi_s} \right) \quad \forall s, \xi_s \quad (50)$$

By solving the DS of the robust model and incorporating the BD cuts, the MP for robust model is subsequently expressed as presented below. The BD pseudocode, previously introduced as Algorithm 1, is used here for the robust model, with the only modification being the  $UB$ , which is now set to the objective value of the DS in each iteration of the algorithm.

$$\min B \quad (51)$$

s.to:

$$\omega'(\xi_s) \geq \sum_t \left( \sum_m \theta_m \bar{g}_{mt \xi_s} - \sum_j \sum_n \sum_q \pi_{jnq} z_{jnq} \bar{u}_{jq t \xi_s} - \sum_i \sum_l \beta_{il} \rho_{is} \bar{t}_{il \xi_s} - \sum_k \sum_n \mu_{kn} w_{kn} \bar{c}_{kt \xi_s} \right) \quad \forall s, \xi_s \quad (52)$$

$$B - (TF + TE + \omega'(\xi_s)) \geq \chi(a(\xi_s) - 1) \quad \forall s, \xi_s \quad (53)$$

$$\sum_{\xi_s} \sum_s \zeta(\xi_s) a(\xi_s) \geq \kappa \quad (54)$$

$$\sum_n \sum_q z_{jnq} \leq 1 \quad \forall j \quad (55)$$

$$\sum_n w_{kn} \leq 1 \quad \forall k \quad (56)$$

$$z_{jnq}, w_{kn} \in \{0, 1\} \quad \forall j, k, q, n \quad (57)$$

## 5.3. Solution algorithm for min-max regret model

In the min-max regret model, prior to solving the main model, it is necessary to solve several stochastic models. These models are employed to calculate the optimal BSC cost value for each disruption scenario  $s \in S$ , define as  $F^s$ . Assuming the values of  $z_{jnq}$ , and  $w_{kn}$  are fixed, the PS of the min-max regret model is equivalent to Eqs. (58)–(59), subject to the additional constraints specified in Eqs. (31)–(40).

$$\min U \quad (58)$$

s.to:

$$U \geq TF + TE + \mathbb{E}_{\xi_s} [SC(\xi_s) + PC(\xi_s) + BC(\xi_s) + IC(\xi_s) + RC(\xi_s)] - F^s \quad \forall s \quad (59)$$

Therefore, the corresponding BD cut can be computed by Eq. (60) as follows:

$$\omega'' \leq \hat{F}_s - \sum_{\xi_s} \sum_t \left( \sum_m \theta_m \bar{g}_{mt \xi_s} - \sum_j \sum_n \sum_q \pi_{jnq} z_{jnq} \bar{u}_{jq t \xi_s} - \sum_i \sum_l \beta_{il} \rho_{is} \bar{t}_{il \xi_s} - \sum_k \sum_n \mu_{kn} w_{kn} \bar{c}_{kt \xi_s} \right) \quad \forall s \quad (60)$$

The MP for the min-max regret model is developed using the dual variables and BD cuts, which are derived from solving the DS of the min-max regret model.

$$\max \omega'' - \sum_j \sum_n \sum_q \delta_{jmq} z_{jmq} - \sum_k \sum_n \sigma_{kn} w_{kn} \quad (61)$$

s.to:

$$\omega'' \leq \hat{F}_s - \sum_{\xi_s} \sum_t \left( \sum_m \theta_m \bar{g}_{mt\xi_s} - \sum_j \sum_n \sum_q \pi_{jmq} z_{jmq} \bar{u}_{jq t \xi_s} - \sum_i \sum_l \beta_{il} \rho_{is} \bar{t}_{il \xi_s} - \sum_k \sum_n \mu_{kn} w_{kn} \bar{c}_{kt \xi_s} \right) \forall s \quad (62)$$

$$\sum_n \sum_q z_{jmq} \leq 1 \forall j \quad (63)$$

$$\sum_n w_{kn} \leq 1 \forall k \quad (64)$$

$$z_{jmq}, w_{kn} \in \{0, 1\} \forall j, k, q, n \quad (65)$$

where  $\hat{F}_s$  is calculated using Algorithm 1 for each disruption scenario  $s \in S$ , in which  $UB$  computed using the Eq. (47). Based on the explanations provided in this section, Algorithm 1 is implemented as the BD algorithm for solving proposed min-max regret model. For this model  $UB$  is calculated using Eq. (66), in which  $F_{DS}^r$  represents the objective value of the DS of the min-max regret model in each iteration of the algorithm.

$$UB = \max_s \sum_j \sum_n \sum_q \delta_{jmq} z_{jmq} + \sum_k \sum_n \sigma_{kn} w_{kn} + F_{DS}^r - \hat{F}_s \quad (66)$$

#### 5.4. Accelerated technique

To enhance the efficiency of solving the model using the BD algorithm, an acceleration technique is introduced in this section. To solve the proposed models with this technique, the BD algorithm is first applied with a relaxed linear programming version of each model. Upon convergence of the BD bounds, the resulting cuts are retained. Subsequently, the original algorithm is executed using the initial binary variables along with the cuts generated in the previous phase.

For instance, when solving the stochastic model using Algorithm 1, the binary variables ( $z_{jmq}$  and  $w_{kn}$ ) are initially relaxed, and the algorithm is executed. After convergence, the generated cuts are integrated into the original algorithm, where  $z_{jmq}$  and  $w_{kn}$  are treated as binary. Algorithm 1 is then re-executed to determine the optimal solution of the stochastic model. Using the same approach, the acceleration technique is also applicable to robust and min-max regret models.

### 6. Computational experiments

In this section, the performance of proposed models and algorithms is investigated. For this purpose, the Iran-related data is collected, and the case study is expanded. The planning horizon for the case study is one year, consisting of four time periods, with each period representing one season (three months).

A workstation computer with Intel Core i7-8700 K CPU (3.70 GHz), with 32.0 GB of RAM, is used for the implementation of this model in GAMS 24.1 environment with CPLEX 12.5 solver.

#### 6.1. Case study

Since sufficient infrastructure for biofuel production has yet to be developed in Iran, in this paper, the BSC design for the biofuel supply equivalent to 5 % of the gasoline demand of the provinces of Iran is carried out. Based on the information published by Iran's Ministry of Petroleum, the annual gasoline consumption in Iran is close to 10.2 billion gallons per year in 2022. The information related to the amount

of gasoline demand in each region is extracted from the data of Iran's Ministry of Petroleum.

Since various types of biomass can be used for biofuel production by using advanced conversion facilities (Fattahi and Govindan, 2018), in this study, only one type of conversion technology is assumed. Wheat straw, barley straw, and corn stover are considered the required biomass for biofuel production. The amount of available biomass is determined using the data published by the Ministry of Agricultural Jihad of Iran. Biofuel to the biomass conversion rate for wheat straw, barley straw, and corn stover equals 90, 120, and 81 gallons per ton, respectively (Fattahi and Govindan, 2018; Panahi et al., 2020).

Biorefineries' nominal capacities are assumed to be 50, 120, and 200 million gallons per year (MGY), with corresponding annualized investment costs of 21.85, 41.95, and 54.53 million dollars, respectively. Additionally, biofuel storage facilities can be established with capacities of 50, 100, and 200 thousand barrels, at annualized costs of 0.765, 1.26, and 2.01 million dollars, respectively (Huang et al., 2014). These estimates are based on a 20-year project horizon and a 10 % interest rate.

The final customers considered in this research are 15 provinces in Iran, each accounting for at least 2 % of the total fuel demand. Biomass suppliers are identified in 16 provinces with adequate biomass availability. Based on expert recommendations, potential sites for establishing biorefineries must meet two criteria: (1) the province's annual biomass production must constitute at least 5 % of the total annual available biomass, and (2) the province must possess the necessary infrastructure to support biorefinery development (Fattahi and Govindan, 2018). Under these conditions, 10 provincial centers namely, (1) Arak, (2) Esfahan, (3) Ahvaz, (4) Tabriz, (5) Fars, (6) Kerman, (7) Kermanshah, (8) Mashhad, (9) Tehran, and (10) Yazd are identified as candidate locations for biorefineries and storage facilities. The geographical scope of the problem is illustrated in Fig. 4.

The calculation of transportation costs for biofuel and biomass depends on both the distance between provincial centers in Iran and the applicable fare rate per kilometer. Specifically, the transportation cost is determined by multiplying the distance between two provincial centers by the fare rate for each entity per kilometer. For biomass transportation, the fare rate is influenced by specific characteristics of each biomass type, such as moisture content and bulk density. Additionally, the transportation capacities are assumed to be 25 tons for biomass

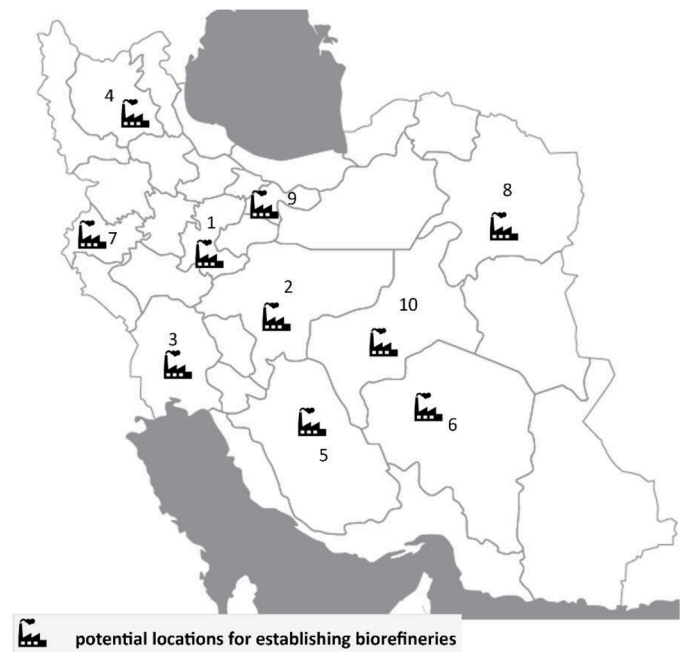


Fig. 4. Potential locations for establishing biorefineries.

trucks and 8,000 gallons for biofuel trucks.

The effects of disruptions on biomass availability are quantified using statistical data on floods and frost incidents in Iran's provinces, as published by the Iranian Disaster Management Organization. The disrupted biomass availability is calculated by adjusting its nominal amount according to the percentage impact of each disruption. Fluctuations in biomass price, independent of disruptions, are modeled using historical data and the K-means clustering method. To determine biomass prices across scenarios, an initial dataset is collected, and the K-means clustering algorithm is applied with K-values of 5, 10, and 15. The algorithm identifies the optimal candidate from each cluster, which is then selected as the representative biomass price scenario.

## 6.2. Results for stochastic model

This section presents the results of the stochastic model on case study data. First, the performance of the proposed BD algorithm is evaluated. For this purpose, several test problems of different sizes are solved using CPLEX, the BD algorithm, and accelerated BD algorithm. The stopping criterion of the BD algorithm is the equality of the upper and lower bounds of this algorithm. The time limit for each solving method is 2 hours.

The results of the stochastic model are summarized in Table 3. The columns, arranged from left to right, denote the number of disruption scenarios, biomass price scenarios, suppliers, potential biorefinery locations, potential storage facility locations, and customer points, followed by the number of variables and constraints, the CPU time (in seconds) with the optimality gap percentage and the optimal objective value (in dollars).

As indicated by the results in Table 3, for test problems with an equal number of disruption and biomass price scenarios, the CPU time exhibits a noticeable increase with the expansion of the problem's geographical scope. This trend is primarily attributed to the increase in the number of integer variables within the model, which significantly impacts computational complexity.

**Table 3**  
Computational result for stochastic model.

Test problem						Number of variables		Number of constraints	CPU times (optimality gap percentage)			Optimal objective value
$ S $	$ \Xi $	$ I $	$ J $	$ K $	$ M $	Binary variables	Continues variables		CPLEX	BD	Accelerated BD	
3	5	5	2	2	5	12	1935	1264	5 (0)	5 (0)	10 (0)	3.2469E+8
			4	4	10	24	6450	2528	9 (0)	19 (0)	19 (0)	9.8779E+8
			6	6	12	36	11340	3342	21 (0)	29 (0)	31 (0)	1.1495E+9
			8	8	14	48	17550	4151	25 (0)	53 (0)	41 (0)	1.1437E+9
		10	10	10	15	60	24420	4910	624 (0)	588 (0)	505 (0)	1.0500E+9
			5	2	2	5	12	3870	5 (0)	5 (0)	5 (0)	3.2473E+8
			4	4	10	24	12900	5048	17 (0)	22 (0)	31 (0)	9.8785E+8
			6	6	12	36	22680	6672	50 (0)	56 (0)	52 (0)	1.1496E+9
			8	8	14	48	35100	8296	73 (0)	83 (0)	68 (0)	1.1438E+9
			10	10	15	60	48840	9800	7084 (0)	3128 (0)	1082 (0)	1.0501E+9
		15	5	2	2	5	12	5805	6 (0)	6 (0)	5 (0)	3.2481E+8
			4	4	10	24	19350	7568	15 (0)	21 (0)	22 (0)	9.8799E+8
			6	6	12	36	34020	10002	95 (0)	56 (0)	49 (0)	1.1497E+9
			8	8	14	48	52650	12436	488 (0)	305 (0)	118 (0)	1.1439E+9
			10	10	15	60	73260	14690	- (4.5)	2077 (0)	1262 (0)	1.0504E+9
	5	5	2	2	5	12	3225	2104	4 (0)	6 (0)	6 (0)	3.2324E+8
			4	4	10	24	10750	4208	12 (0)	23 (0)	22 (0)	9.6797E+8
			6	6	12	36	18900	5562	45 (0)	45 (0)	49 (0)	1.1277E+9
			8	8	14	48	29250	6919	65 (0)	70 (0)	66 (0)	1.1437E+9
		10	10	10	15	60	40700	8170	971 (0)	555 (0)	308 (0)	9.9819E+8
			5	2	2	5	12	6450	5 (0)	5 (0)	6 (0)	3.2327E+8
			4	4	10	24	21500	8408	26 (0)	27 (0)	29 (0)	9.6803E+8
			6	6	12	36	37800	11112	67 (0)	52 (0)	48 (0)	1.1278E+9
			8	8	14	48	58500	13816	51 (0)	60 (0)	67 (0)	1.1438E+9
			10	10	15	60	81400	16320	- (2.7)	952 (0)	904 (0)	9.9830E+8
		15	5	2	2	5	12	9675	5 (0)	5 (0)	7 (0)	3.4562E+8
			4	4	10	24	32250	12608	44 (0)	45 (0)	45 (0)	9.6817E+8
			6	6	12	36	56700	16662	250 (0)	91 (0)	73 (0)	1.1280E+9
			8	8	14	48	87750	20716	312 (0)	196 (0)	158 (0)	1.1439E+9
			10	10	15	60	122100	24470	- (4.4)	644 (0)	319 (0)	9.9855E+8

The results presented in Table 3 indicate that for problems with smaller geographical dimensions, the CPLEX method performs slightly better. However, as the problem dimensions and the number of scenarios increase, the proposed algorithms demonstrate superior performance. This advantage becomes increasingly evident with the growth in both the problem size and the number of scenarios. Furthermore, the results clearly demonstrate that the Benders algorithm, when augmented with the acceleration technique, achieves significantly improved performance. This advantage is particularly evident in large-scale problems, where CPLEX fails to solve the model within the specified 2-hour time limit, as indicated by the dash "-" in the Table 3.

## 6.3. Results for robust model

In this section, a comparative analysis of the robust model results is presented. To achieve this, the robust model is solved using three distinct algorithms: CPLEX, BD, and Accelerated BD. The corresponding results are provided in Table 4. The column arrangement in Table 4 is consistent with that of Table 3. This section considers a confidence level of  $\kappa = 0.85$ .

As shown in Table 4, the CPU time for the robust model using the CPLEX, BD, and Accelerated BD algorithms are, on average, longer than those for the corresponding stochastic model test problems across all algorithms. Additionally, in some test problems, the robust model's optimal solution could not be achieved within the designated time limit. In contrast, for the stochastic model, at least one of the algorithms successfully computed the optimal solution in all test problems.

The results for the robust model, as reported in Table 4, indicate that both the geographical dimensions and the number of scenarios have a direct impact on the solution time for the test problems. In other words, for problems with the same number of scenarios, an increase in geographical dimensions leads to longer solution times. Similarly, for problems with the same geographical dimensions, an increase in the number of scenarios results in higher CPU times.

In the majority of test problems, where optimal solutions were



**Table 4**  
Computational result for robust model.

Test problem						Number of variables		Number of constraints	CPU times (optimality gap)			Optimal objective value
$ S $	$ \Xi $	$ I $	$ J $	$ K $	$ M $	Binary variables	Continues variables		CPLEX	BD	Accelerated BD	
3	5	5	2	2	5	27	1935	1280	10 (0)	16 (0)	17 (0)	3.6126E+8
		10	4	4	10	39	6450	2544	17 (0)	25 (0)	24 (0)	9.9867E+8
		12	6	6	12	51	11340	3358	103 (0)	90 (0)	67 (0)	1.1783E+9
		14	8	8	14	63	17550	4167	740 (0)	228 (0)	190 (0)	1.1483E+9
	10	16	10	10	15	75	24420	4926	- (6.4)	- (3.5)	6749 (0)	1.0493E+9
		5	2	2	5	42	3870	2555	30 (0)	49 (0)	60 (0)	3.6150E+8
		10	4	4	10	54	12900	5079	217 (0)	120 (0)	84 (0)	9.9906E+8
		12	6	6	12	66	22680	6703	748 (0)	188 (0)	65 (0)	1.1912E+9
	15	14	8	8	14	78	35100	8327	- (1.5)	780 (0)	301 (0)	1.1696E+9
		16	10	10	15	90	48840	9831	- (7.2)	- (3.6)	- (1.6)	-
		5	2	2	5	57	5805	3830	55 (0)	51 (0)	67 (0)	3.6173E+8
		10	4	4	10	69	19350	7614	596 (0)	152 (0)	86 (0)	1.0068E+9
	5	12	6	6	12	81	34020	10048	4776 (0)	1005 (0)	391 (0)	1.1791E+9
		14	8	8	14	93	52650	12482	- (14.6)	902 (0)	393 (0)	1.1616E+9
		16	10	10	15	105	73260	14736	- (24.1)	- (18)	- (3.2)	-
		5	2	2	5	37	3225	2130	5 (0)	14 (0)	21 (0)	3.4515E+8
5	5	10	4	4	10	49	10750	4234	131 (0)	105 (0)	82 (0)	9.9839E+8
		12	6	6	12	61	18900	5588	477 (0)	184 (0)	162 (0)	1.1781E+9
		14	8	8	14	73	29250	6945	618 (0)	391 (0)	357 (0)	1.1483E+9
		16	10	10	15	85	40700	8196	- (9.7)	- (9.5)	- (3.3)	-
	10	5	2	2	5	62	6450	4255	152 (0)	140 (0)	144 (0)	3.4537E+8
		10	4	4	10	74	21500	8459	558 (0)	255 (0)	120 (0)	9.9808E+8
		12	6	6	12	86	37800	11163	- (4.3)	579 (0)	204 (0)	1.1781E+9
		14	8	8	14	98	58500	13867	- (11.5)	- (5.7)	2620 (0)	1.1489E+9
	15	16	10	10	15	110	81400	16371	- (22)	- (11.1)	- (3.2)	-
		5	2	2	5	87	9675	6380	104 (0)	70 (0)	64 (0)	3.4562E+8
		10	4	4	10	99	32250	12684	2748 (0)	654 (0)	218 (0)	9.9806E+8
		12	6	6	12	111	56700	16738	- (9.5)	2789 (0)	740 (0)	1.1777E+9
	5	14	8	8	14	123	87750	20792	- (16)	- (10.4)	6380 (0)	1.1494E+9
		16	10	10	15	135	122100	24546	- (26.1)	- (19.9)	- (7.5)	-

obtained within the designated time limit, BD-based algorithms exhibited significantly superior performance compared to the CPLEX algorithm. Additionally, the Accelerated BD algorithm, similar to its

performance in solving stochastic model test problems, outperformed the BD algorithm in solving the robust model. Overall, the CPLEX algorithm failed to solve 40 % of the test problems, while the failure rates

**Table 5**  
Computational result for min-max regret model.

Test problem						Number of variables		Number of constraints	CPU times (optimality gap)			Optimal objective value
$ S $	$ \Xi $	$ I $	$ J $	$ K $	$ M $	Binary variables	Continues variables		CPLEX	BD	Accelerated BD	
3	5	5	2	2	5	12	1935	1267	2 (0)	7 (0)	11 (0)	2.1467E+7
		10	4	4	10	24	6450	2531	15 (0)	28 (0)	30 (0)	2.8009E+7
		12	6	6	12	36	11340	3345	121 (0)	77 (0)	69 (0)	4.0733E+7
		14	8	8	14	48	17550	4154	437 (0)	100 (0)	218 (0)	4.9777E+7
	10	16	10	10	15	60	24420	4913	1998 (0)	778 (0)	656 (0)	6.8475E+7
		5	2	2	5	12	3870	2527	5 (0)	11 (0)	11 (0)	2.1467E+7
		10	4	4	10	24	12900	5051	51 (0)	38 (0)	38 (0)	2.8000E+7
		12	6	6	12	36	22680	6675	68 (0)	69 (0)	66 (0)	4.0733E+7
	15	14	8	8	14	48	35100	8301	2218 (0)	312 (0)	365 (0)	4.9777E+7
		16	10	10	15	60	48840	9803	- (2.6)	3220 (0)	3389 (0)	6.8475E+7
		5	2	2	5	12	5805	3787	10 (0)	13 (0)	13 (0)	2.1467E+7
		10	4	4	10	24	19350	7571	50 (0)	49 (0)	42 (0)	2.8000E+7
	5	12	6	6	12	36	34020	10005	338 (0)	60 (0)	67 (0)	4.0733E+7
		14	8	8	14	48	52650	12436	- (3.8)	420 (0)	461 (0)	4.9777E+7
		16	10	10	15	60	73260	14693	- (9.2)	4008 (0)	3910 (0)	6.8475E+7
		5	2	2	5	12	3225	2109	10 (0)	15 (0)	15 (0)	2.3293E+7
5	5	10	4	4	10	24	10750	4213	50 (0)	39 (0)	55 (0)	2.7700E+7
		12	6	6	12	36	18900	5567	224 (0)	117 (0)	122 (0)	4.1401E+7
		14	8	8	14	48	29250	6921	1402 (0)	617 (0)	699 (0)	7.0590E+7
		16	10	10	15	60	40700	8175	- (3.3)	6621 (0)	4440 (0)	6.8415E+7
	10	5	2	2	5	12	6450	4209	10 (0)	15 (0)	17 (0)	2.3293E+7
		10	4	4	10	24	21500	8413	412 (0)	50 (0)	61 (0)	2.7700E+7
		12	6	6	12	36	37800	11122	1454 (0)	120 (0)	142 (0)	4.1401E+7
		14	8	8	14	48	58500	13821	- (4.1)	344 (0)	357 (0)	6.2027E+7
	15	16	10	10	15	60	81400	16325	- (9.5)	- (3.8)	7024 (0)	6.8415E+7
		5	2	2	5	12	9675	6309	10 (0)	17 (0)	17 (0)	2.3293E+7
		10	4	4	10	24	32250	12613	398 (0)	55 (0)	58 (0)	2.7700E+7
		12	6	6	12	36	56700	16667	2446 (0)	79 (0)	133 (0)	4.1401E+7
	5	14	8	8	14	48	87750	20721	- (9.7)	361 (0)	452 (0)	7.8652E+7
		16	10	10	15	60	122100	24475	- (17)	- (12.4)	7115 (0)	6.8415E+7

for the BD and Accelerated BD algorithms were 27 % and 17 %, respectively, highlighting the superior efficiency of these two approaches.

#### 6.4. Results for min-max regret model

In this section, to evaluate the performance of the CPLEX algorithm and the proposed BD-based algorithms in solving the min-max regret model, several test problems are solved. The results necessary for analyzing the performance of the algorithms are presented in Table 5. The columns of this table are structured similarly to those in Table 3.

The solutions reported in Table 5 indicate that the solution time for the min-max regret model, similar to the stochastic and robust models, increases with the geographical dimensions and the number of scenarios. Furthermore, the optimal solution for all test problems was obtained by at least one algorithm. Notably, the accelerated BD-based algorithm successfully solved all test problems, whereas CPLEX and BD algorithm failed to solve 27 % and 7 % of the test problems, respectively.

In solving the min-max regret model, both the BD algorithm and the accelerated BD algorithm outperformed CPLEX. Moreover, in most test problems, the BD algorithm demonstrated better performance than the accelerated BD algorithm. However, the accelerated BD algorithm showed superior performance in test problems with the largest geographical dimensions. Therefore, for large-scale problems, the accelerated BD algorithm performs more effectively.

#### 6.5. Models results comparison

This section provides a comparative analysis of strategic decisions derived from the three proposed models and evaluates their impact on the respective objective functions. Specifically, the strategic decisions determined by each model are fixed and subsequently applied to the other models to assess the resulting objective function values. In this part of the study, "Test problems 1 to 5" correspond to cases with increasing geographical scale, as outlined in Table 3. For example, test problem 5 involves 16 suppliers, 10 candidate facility locations, and 15 customers. Each test problem includes 5 uncertainty scenarios and 3 disruption scenarios.

The results of this analysis are presented in Table 6. The columns in Table 6, listed from left to right, represent the type of model under analysis, the locations and capacity of biorefineries, the locations and capacity of storage facilities, the expected total cost of BSC (the objective function value for the stochastic model), the target threshold total cost (the objective function value for the robust model), and maximum regret (the objective function value for the min-max regret model). For example, the value 1.0147E+09 listed under the "Target threshold cost" column in the row associated with the "Stochastic model" indicates the

objective function value of the robust model, calculated using the strategic decisions derived from the stochastic model.

Notably, the objective function values in Table 6 are expressed in dollars, and the location indices correspond to the candidate location numbers introduced in Section 6.1. The numbers in parentheses next to each facility location represent the capacity levels of the facilities, with values 1 to 3 indicating low, medium, and high capacities, respectively.

As anticipated, the stochastic model, robust model, and min-max regret model achieve the optimal values for expected cost, target threshold cost, and max regret, respectively. Given that each model exhibits the best performance with respect to its respective criterion, a meaningful comparison can only be made between the performance of the other models within the context of these specific criteria. This section is dedicated to conducting such comparative analyses.

The results presented in Table 6 indicate that each of the proposed models follows a different approach in determining strategic decisions, which naturally leads to varying outcomes. Overall, the min-max regret model exhibits better performance, as its solutions show smaller deviations from the optimal responses provided by the stochastic and robust models. This suggests that the min-max regret approach offers a more balanced decision-making framework under uncertainty by combining cost-effectiveness with acceptable levels of robustness.

The numerical results, averaged across the 5 analyzed test problems, reveal that the expected cost in the robust and min-max regret models is 2.15 % and 0.47 % higher, respectively, than that of the stochastic model. This suggests that the stochastic model performs slightly better in terms of minimizing average cost. However, when considering performance under uncertainty, the target threshold cost of the stochastic and min-max regret models is 0.94 % and 0.61 % higher, respectively, than that of the robust model. This indicates that the robust model is more conservative and better suited to handle unfavorable scenarios. Moreover, the maximum regret values in the stochastic and robust models are 10.09 % and 13.54 % greater, respectively, than in the min-max regret model. These findings underscore the capability of the min-max regret model to provide more balanced and resilient decisions under varying uncertainty scenarios.

Overall, the results demonstrate that each modeling approach reflects a different trade-off between cost-efficiency and robustness. The stochastic model provides the most cost-effective solution under known probability distributions, while the robust model emphasizes protection against unfavorable outcomes by favoring fewer but higher-capacity facilities. The min-max regret model, on the other hand, balances these two priorities by delivering reliable decisions with moderate costs and minimized regret. As such, it offers a practical and resilient alternative in situations where scenario probabilities are unknown or decision-makers aim to mitigate the risk of suboptimal outcomes.

**Table 6**  
Comparison of tree proposed models.

	Problem	Open biorefineries (Capacity level)	Open storage (Capacity level)	Expected cost	Target threshold cost	Max regret
Test Problem 1	Stochastic model	1(2)	1(2)	3.2469E+08	3.6126E+08	2.1467E+07
	Robust model	1(2)	1(2)	3.2469E+08	3.6126E+08	2.1467E+07
	Min-max regret model	1(2)	1(2)	3.2469E+08	3.6126E+08	2.1467E+07
Test Problem 2	Stochastic model	1(3)	1(3)	9.8779E+08	1.0147E+09	4.1020E+07
	Robust model	1(1),2(1)	1(1),2(1)	9.9734E+08	9.9867E+08	2.9190E+07
	Min-max regret model	3(1),4(1)	3(1),4(1)	9.9450E+08	1.0020E+09	2.8009E+07
Test Problem 3	Stochastic model	1(3)	1(3)	1.1495E+09	1.1978E+09	4.0733E+07
	Robust model	1(1),5(1)	1(1),5(1)	1.1818E+09	1.1783E+09	5.0816E+07
	Min-max regret model	1(3)	1(3)	1.1495E+09	1.1978E+09	4.0733E+07
Test Problem 4	Stochastic model	2(1),4(1),7(1)	2(1),4(1),7(1)	1.1437E+09	1.1558E+09	5.0625E+07
	Robust model	1(1),5(1),7(1)	1(1),5(1),7(1)	1.1485E+09	1.1483E+09	5.0606E+07
	Min-max regret model	3(1),5(1),7(1)	3(1),5(1),7(1)	1.1529E+09	1.1530E+09	4.9777E+07
Test Problem 5	Stochastic model	1(1),4(1),7(1),8(1)	1(1),4(1),7(1),8(1)	1.0500E+9	1.0574E+9	7.0070E+7
	Robust model	5(1),9(3)	5(1),9(3)	1.1188E+9	1.0493E+9	9.3825E+7
	Min-max regret model	3(1),5(1),7(1),8(1)	3(1),5(1),7(1),8(1)	1.0591E+9	1.0556E+9	6.8475E+7

### 6.6. Analyzing the impact of biomass availability

In this section, the performance of the proposed models is evaluated by analyzing the impact of variations in biomass availability. The findings from this analysis can serve as a managerial insight for planning and expanding biomass cultivation and production. In the conducted sensitivity analyses, "test problems 1 to 4" refer to problems ranging from the smallest to the largest geographical scales have been introduced in Table 3, respectively. For instance, test problem 4 represents a case with 14 suppliers, 8 candidate locations for facility establishment, and 14 customers. In these test problems, the number of uncertainty and disruption scenarios are set to 5 and 3, respectively.

Fig. 5 illustrates the sensitivity analysis results of the available biomass parameter within the stochastic model. In this section, sensitivity analyses were conducted on test problems by assuming changes of -10 %, -5 %, +5 %, +10 %, and +15 % in the available biomass. As depicted in Fig. 5, it is evident that an increase in available biomass leads to a reduction in BSC costs. The primary reason for this cost reduction is the increased production of biofuels and the decreased reliance on imports. In a similar manner, the robust model also demonstrates that an increase in the availability of biomass, leading to reduced biofuel import costs, results in a decrease in the target threshold of the BSC total cost, as illustrated in Fig. 6.

Moreover, in the solutions obtained from the min-max regret model, an increase in the available biomass exhibits a notable trend. In the examined test problems, a rise in available biomass generally leads to an increase in biofuel production. When this higher production is achieved through the addition of new facilities or by selecting facilities with greater capacity, the result is higher capital investment costs, which in turn lead to an increase in the value of min-max regret. In contrast, when the additional production is achieved solely due to the increased availability of biomass, without altering the number or capacity of facilities, the objective value of the min-max regret model tends to decrease. This pattern is clearly illustrated in Fig. 7.

A more detailed analysis of the results indicates that, with the exception of Test Problem 1, where the biomass demand is relatively low, an increase in biomass availability generally leads to a higher overall production capacity. This increase is realized in one of two ways: either by keeping the number of selected biorefineries constant while assigning them higher capacity levels, or by selecting more biorefineries with relatively lower capacities. This outcome reflects the cost-effectiveness of domestic biofuel production compared to imports. As the biomass availability increase, the models tend to prioritize

expanding local production, which not only reduces reliance on imports but also lowers the total cost of the BSC and enhances system robustness.

## 7. Managerial insights

The findings reveal that each proposed model results in a distinct BSC configuration, shaped by its underlying decision-making logic and risk-handling strategy. Therefore, selecting the appropriate model depends on the decision-maker's risk tolerance, operational priorities, and the availability of reliable data.

Risk-neutral planners, who can access sufficient historical data and estimate the probability distributions of uncertain parameters, may favor the stochastic model for its ability to generate cost-effective supply chain structures under average conditions. In contrast, risk-averse decision-makers, particularly those operating in volatile or disruption-prone environments, may prefer the robust model, which ensures feasibility at a specified confidence level and minimizes the target threshold cost, thereby enhancing system resilience.

Where precise probabilistic information is unavailable or difficult to obtain, the min-max regret model provides a balanced solution that minimizes the maximum regret across all scenarios. This approach is especially appropriate for risk-averse decision-makers who seek cost-effective and resilient supply chain designs in the absence of reliable data. By incorporating this model alongside stochastic and robust counterparts, the framework enables decision-makers to choose a method aligned with their risk preferences and data availability.

Furthermore, the sensitivity analysis demonstrates that increasing the availability of biomass, whether through geographic diversification of suppliers or enhanced domestic cultivation, can significantly reduce overall supply chain costs. This is primarily achieved by decreasing dependency on costly biofuel imports and increasing local production capacity. The benefits of this strategy are particularly evident in larger-scale scenarios, where the flexibility to adjust facility capacity or establish new sites can lead to enhanced resilience and adaptability.

In practical terms, these insights suggest that investing in local biomass cultivation, coupled with choosing a modeling approach aligned with the organization's risk profile, can create more stable and efficient supply chains. Policymakers and planners are therefore encouraged to consider these factors in long-term infrastructure investments and policy frameworks for sustainable bioenergy development.

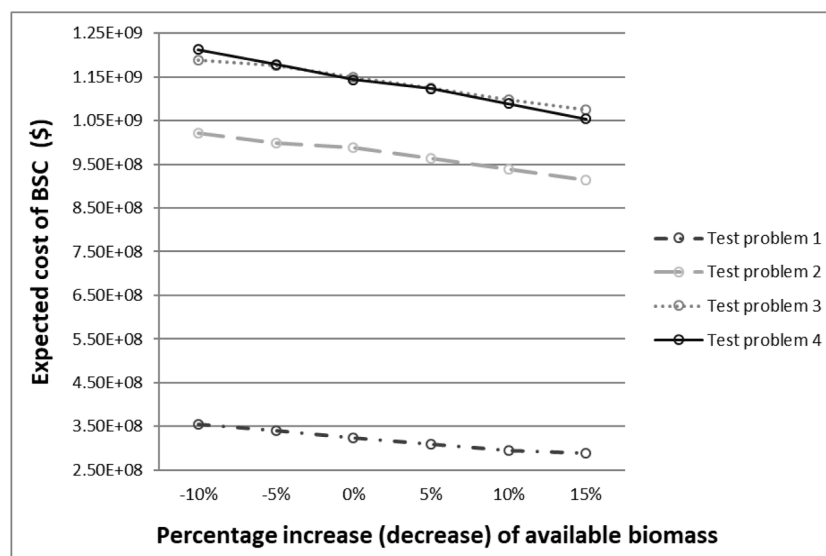


Fig. 5. The sensitivity of stochastic model's objective function on biomass availability.

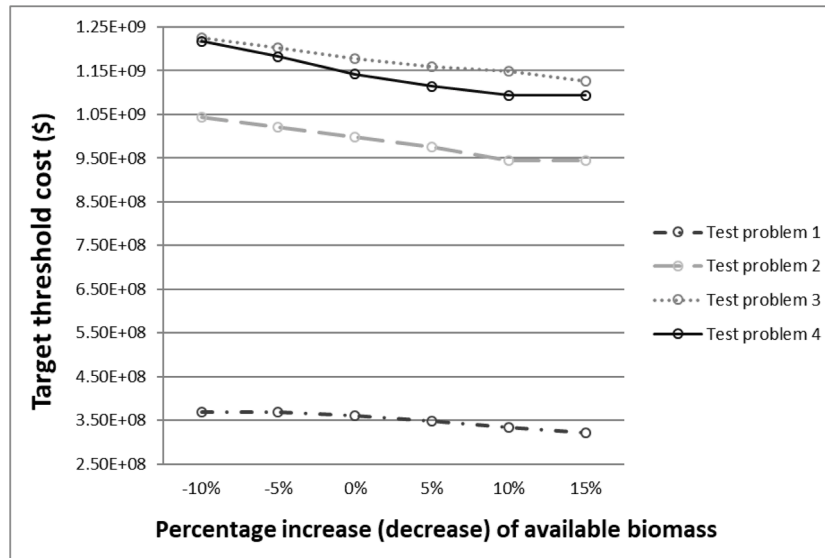


Fig. 6. The sensitivity of robust model's objective function on biomass availability.

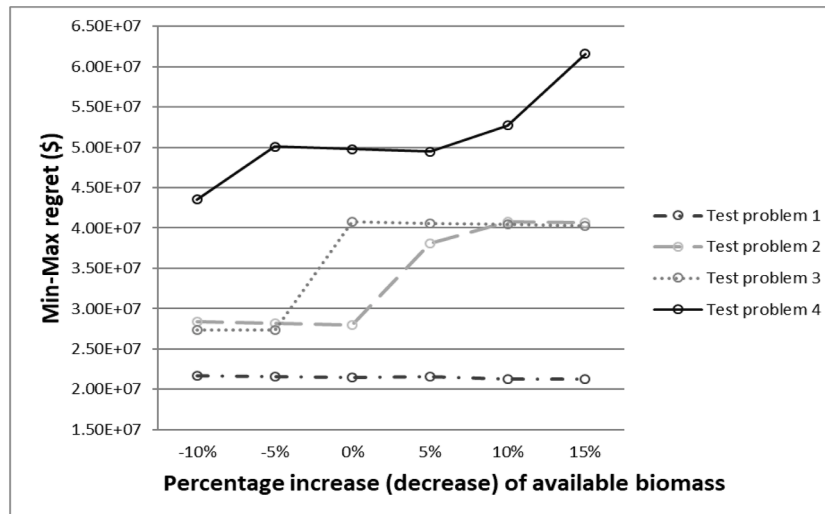


Fig. 7. The sensitivity of min-max regret model's objective function on biomass availability.

## 8. Conclusion

This study developed a comprehensive and resilient framework for the design of BSCs under both uncertainty and disruption. To accommodate different risk attitudes and decision-making preferences, three mathematical optimization models were proposed: (1) the stochastic model, which aims to minimize the expected total cost by considering the probabilistic nature of uncertain parameters; (2) the robust optimization model, which minimizes system costs while ensuring feasibility across all scenarios within a defined uncertainty set and confidence level; and (3) the min-max regret model, which seeks to limit the maximum regret associated with not selecting the optimal decision, offering a robust strategy when the probability distribution of uncertain parameters is unknown.

In this study, both biomass availability and biomass price are treated as uncertain parameters to reflect real-world supply and market conditions. Recognizing the relationship between biomass availability and its market price, a linear pricing function is employed, wherein the biomass price increases as availability decreases. To enhance the realism of this relationship and capture broader market dynamics, an additional

uncertainty term, as error function, is incorporated, reflecting the influence of external factors such as demand fluctuations and competition.

To efficiently solve the proposed models, a BD algorithm enhanced with acceleration technique was developed to reduce computational time and alleviate solution complexity. The framework was validated through a real-world case study based on data from Iran, designed to assess the simultaneous impact of uncertainty and disruption on the BSC network. The computational results confirm the effectiveness of the proposed solution method, with the enhanced BD algorithm consistently outperforming the CPLEX solver in terms of solution speed. Notably, in instances where CPLEX fails to obtain a solution within the time limit, the BD algorithm successfully provides high-quality solutions within a reasonable computational period.

The results show that each of the proposed models leads to a different BSC structure due to its specific decision-making criterion. As a result, there is a trade-off between cost efficiency, robustness, and decision reliability, making each model suitable for different planning needs and levels of uncertainty. The stochastic model proves to be the most cost-effective when the probability distributions of uncertain parameters are known, while the robust model seeks to ensure operations remain



viable within a defined confidence level, strengthening supply chain resilience, though often requiring higher expected costs. Meanwhile, the min-max regret model offers a suitable option for risk-averse decision-makers, as it balances cost-effectiveness with resilience, even in the absence of precise probabilistic data.

Insights from the sensitivity analyses highlight the strategic importance of increasing biomass availability, which reduces dependence on imports, enhances production flexibility, and strengthens system resilience. These benefits are especially important in large-scale systems, emphasizing the value of increasing domestic biomass production. These findings provide actionable guidance for supply chain planners aiming to balance cost, resilience, and adaptability in uncertain environments.

In the case of future studies, other uncertain parameters can be considered for modeling the BSC with proposed models. Parameters such as the cost of advertising for the expansion of biofuel consumption and its demand, as well as the expansion of alternative fuels and biofuel demand, can be formulated simultaneously with proposed models. Furthermore, these models can incorporate considerations related to sustainability, including social and environmental issues.

### CRedit authorship contribution statement

**Mohammad Ali Karimi:** Writing – original draft, Software, Methodology, Formal analysis, Data curation. **Hossein Neghabi:** Writing – review & editing, Supervision, Methodology, Conceptualization.

### Declaration of competing interest

The authors declare that they have no known competing financial interests or personal relationships that could have appeared to influence the work reported in this paper.

### Data availability

The data that has been used is confidential.

### References

- Aboytes-Ojeda, M., Castillo-Villar, K.K., Cardona-Valdés, Y., 2022. Bi-objective stochastic model for the design of biofuel supply chains incorporating risk. *Expert. Syst. Appl.* 202, 117285.
- Ahmadvand, S., Sowlati, T., 2022. A robust optimization model for tactical planning of the forest-based biomass supply chain for syngas production. *Comput. Chem. Eng.* 159, 107693.
- Alizadeh, M., Ma, J., Marufuzzaman, M., Yu, F., 2019. Sustainable olefin supply chain network design under seasonal feedstock supplies and uncertain carbon tax rate. *J. Clean. Prod.* 222, 280–299.
- Allman, A., Lee, C., Martín, M., Zhang, Q., 2021. Biomass waste-to-energy supply chain optimization with mobile production modules. *Comput. Chem. Eng.* 150, 107326.
- Aranguren, M., Castillo-Villar, K., 2022. Bi-objective stochastic model for the design of large-scale carbon footprint conscious co-firing biomass supply chains. *Comput. Ind. Eng.* 171, 108352.
- Bairamzadeh, S., Pishvae, M.S., Saidi-Mehrabad, M., 2016. Multiobjective robust possibilistic programming approach to sustainable bioethanol supply chain design under multiple uncertainties. *Ind. Eng. Chem. Res.* 55 (1), 237–256.
- Bang, C., Vitina, A., Gregg, J.S., Lindboe, H.H., 2013. Analysis of Biomass Prices FUTURE DANISH PRICES FOR STRAW, WOOD CHIPS AND WOOD PELLETS “FINAL REPORT”. EA Energy Analyses Frederiksholms Kanal 4, 3. th.
- Ben-Tal, A., Golany, B., Nemirovski, A., Vial, J.-P., 2005. Retailer-supplier flexible commitments contracts: a robust optimization approach. *Manuf. Serv. Oper. Manag.* 7 (3), 248–271.
- Bertsimas, D., Sim, M., 2004. The price of robustness. *Oper. Res.* 52 (1), 35–53.
- Cao, J.X., Zhang, Z., Zhou, Y., 2021. A location-routing problem for biomass supply chains. *Comput. Ind. Eng.* 152, 107017.
- Chen, C.-W., Fan, Y., 2012. Bioethanol supply chain system planning under supply and demand uncertainties. *Transport. Res. Part E* 48 (1), 150–164.
- Chen, Z., Sim, M., Xiong, P., 2020. Robust stochastic optimization made easy with RSOME. *Manage. Sci.* 66 (8), 3329–3339.
- Cundiff, J.S., Dias, N., Serali, H.D., 1997. A linear programming approach for designing a herbaceous biomass delivery system. *Bioresour. Technol.* 59 (1), 47–55.
- Dal-Mas, M., Giarola, S., Zamboni, A., Bezzo, F., 2011. Strategic design and investment capacity planning of the ethanol supply chain under price uncertainty. *Biomass Bioenergy* 35 (5), 2059–2071.
- Dupačová, J., Gröwe-Kuska, N., Römisch, W., 2003. Scenario reduction in stochastic programming. *Math. Program.* 95, 493–511.
- Eksioglu, S.D., Acharya, A., Leightley, L.E., Arora, S., 2009. Analyzing the design and management of biomass-to-biorefinery supply chain. *Comput. Ind. Eng.* 57 (4), 1342–1352.
- Fattahi, M., Govindan, K., 2018. A multi-stage stochastic program for the sustainable design of biofuel supply chain networks under biomass supply uncertainty and disruption risk: a real-life case study. *Transport. Res. Part E* 118, 534–567.
- Ghaderi, H., Pishvae, M.S., Moini, A., 2016. Biomass supply chain network design: an optimization-oriented review and analysis. *Ind. Crops. Prod.* 94, 972–1000.
- Ghelichi, Z., Saidi-Mehrabad, M., Pishvae, M.S., 2018. A stochastic programming approach toward optimal design and planning of an integrated green biodiesel supply chain network under uncertainty: a case study. *Energy* 156, 661–687.
- Gonela, V., Zhang, J., Osmani, A., Onyeaghalala, R., 2015. Stochastic optimization of sustainable hybrid generation bioethanol supply chains. *Transport. Res. Part E* 77, 1–28.
- Gumte, K., Pantula, P.D., Miriyala, S.S., Mitra, K., 2021. Achieving wealth from bio-waste in a nationwide supply chain setup under uncertain environment through data driven robust optimization approach. *J. Clean. Prod.* 291, 125702.
- Habib, M.S., Omair, M., Ramzan, M.B., Chaudhary, T.N., Farooq, M., Sarkar, B., 2022. A robust possibilistic flexible programming approach toward a resilient and cost-efficient biodiesel supply chain network. *J. Clean. Prod.* 366, 132752.
- Habibi, F., Chakraborty, R.K., Abbasi, A., 2023. Towards facing uncertainties in biofuel supply chain networks: a systematic literature review. *Environ. Sci. Pollut. Res.* 30 (45), 100360–100390.
- Huang, Y., Fan, Y., Chen, C.-W., 2014. An integrated biofuel supply chain to cope with feedstock seasonality and uncertainty. *Transport. Sci.* 48 (4), 540–554.
- Kazakci, A., Rozakis, S., Vanderpooten, D., 2007. Energy crop supply in France: a min-max regret approach. *J. Oper. Res. Soc.* 58 (11), 1470–1479.
- Khezerlou, H.S., Vahdani, B., Yazdani, M., 2021. Designing a resilient and reliable biomass-to-biodiesel supply chain under risk pooling and congestion effects and fleet management. *J. Clean. Prod.* 281, 125101.
- Kim, J., Realf, M.J., Lee, J.H., 2011. Optimal design and global sensitivity analysis of biomass supply chain networks for biofuels under uncertainty. *Comput. Chem. Eng.* 35 (9), 1738–1751.
- Kumar, D., Soni, G., Joshi, R., Jain, V., Sohal, A., 2022. Modelling supply chain viability during COVID-19 disruption: a case of an Indian automobile manufacturing supply chain. *Oper. Manag. Res.* 15 (3), 1224–1240.
- Li, Y., Chen, K., Collignon, S., Ivanov, D., 2021. Ripple effect in the supply chain network: forward and backward disruption propagation, network health and firm vulnerability. *Eur. J. Oper. Res.* 291 (3), 1117–1131.
- Lima, C., Batista, M., Relvas, S., Barbosa-Povoa, A., 2023. Optimizing the design and planning of a sugar-bioethanol supply chain under uncertain market conditions. *Ind. Eng. Chem. Res.* 62 (15), 6224–6240.
- Maheshwari, P., Singla, S., Shastri, Y., 2017. Resiliency optimization of biomass to biofuel supply chain incorporating regional biomass pre-processing depots. *Biomass Bioenergy* 97, 116–131.
- Mankiw, N.G., 2021. Principles of economics. Cengage Learning.
- Marufuzzaman, M., Eksioglu, S.D., Hernandez, R., 2014. Environmentally friendly supply chain planning and design for biodiesel production via wastewater sludge. *Transport. Sci.* 48 (4), 555–574.
- Memişoğlu, G., Üster, H., 2021. Design of a biofuel supply network under stochastic and price-dependent biomass availability. *IIE Trans.* 53 (8), 869–882.
- Mousavi Ahranjani, P., Ghaderi, S.F., Azadeh, A., Babazadeh, R., 2020. Robust design of a sustainable and resilient bioethanol supply chain under operational and disruption risks. *Clean. Technol. Environ. Policy* 22, 119–151.
- Mulvey, J.M., Vanderbei, R.J., Zenios, S.A., 1995. Robust optimization of large-scale systems. *Oper. Res.* 43 (2), 264–281.
- Panahi, H.K.S., Dehghani, M., Aghbashlo, M., Karimi, K., Tabatabaei, M., 2020. Conversion of residues from agro-food industry into bioethanol in Iran: an under-valued biofuel additive to phase out MTBE in gasoline. *Renew. Energy* 145, 699–710.
- Paulo, H., Azcue, X., Barbosa-Póvoa, A.P., Relvas, S., 2015. Supply chain optimization of residual forestry biomass for bioenergy production: the case study of Portugal. *Biomass Bioenergy* 83, 245–256.
- Paulo, H., Barbosa-Póvoa, A.P.F., Relvas, S., 2013. Modeling integrated biorefinery supply chains. *Comput. (Long Beach Calif) Aided Chem. Eng.* 32, 79–84.
- Paulo, H., Cardoso-Grilo, T., Relvas, S., Barbosa-Póvoa, A.P., 2017. Designing integrated biorefineries supply chain: combining stochastic programming models with scenario reduction methods. *Comput. (Long Beach Calif) Aided Chem. Eng.* 40, 901–906.
- Paulo, H., Vieira, M., Gonçalves, B.S., Relvas, S., Pinto-Varela, T., Barbosa-Povoa, A.P., 2023. A discrete-event simulation approach to the design and planning of biomass supply chains considering technological learning. *Comput. (Long Beach Calif) Aided Chem. Eng.* 52, 1285–1291.
- Petridis, K., Grigoroudis, E., Arabatzis, G., 2018. A goal programming model for a sustainable biomass supply chain network. *Int. J. Energy Sector Manag.* 12 (1), 79–102.
- Peykani, P., Mohammadi, E., Saen, R.F., Sadjadi, S.J., Rostamy-Malkhalifeh, M., 2020. Data envelopment analysis and robust optimization: a review. *Expert. Syst.* 37 (4), e12534.
- Pishvae, M.S., Razmi, J., Torabi, S.A., 2012. Robust possibilistic programming for socially responsible supply chain network design: a new approach. *Fuzzy. Sets. Syst.* 206, 1–20.
- Poudel, S.R., Marufuzzaman, M., Bian, L., 2016. Designing a reliable bio-fuel supply chain network considering link failure probabilities. *Comput. Ind. Eng.* 91, 85–99.

- Razm, S., Dolgui, A., Hammami, R., Brahimi, N., Nickel, S., Sahebi, H., 2021. A two-phase sequential approach to design bioenergy supply chains under uncertainty and social concerns. *Comput. Chem. Eng.* 145, 107131.
- Saghaei, M., Ghaderi, H., Soleimani, H., 2020. Design and optimization of biomass electricity supply chain with uncertainty in material quality, availability and market demand. *Energy* 197, 117165.
- Salehi, S., Mehrjerdi, Y.Z., Sadegheih, A., Hosseini-Nasab, H., 2022. Designing a resilient and sustainable biomass supply chain network through the optimization approach under uncertainty and the disruption. *J. Clean. Prod.* 359, 131741.
- Samani, M.R.G., Hosseini-Motlagh, S.-M., 2021. A mixed uncertainty approach to design a bioenergy network considering sustainability and efficiency measures. *Comput. Chem. Eng.* 149, 107305.
- Sarkar, B., Mridha, B., Pareek, S., Sarkar, M., Thangavelu, L., 2021. A flexible biofuel and bioenergy production system with transportation disruption under a sustainable supply chain network. *J. Clean. Prod.* 317, 128079.
- Shabani, N., Sowlati, T., 2016. A hybrid multi-stage stochastic programming-robust optimization model for maximizing the supply chain of a forest-based biomass power plant considering uncertainties. *J. Clean. Prod.* 112, 3285–3293.
- Snoeck, A., Udenio, M., Fransoo, J.C., 2019. A stochastic program to evaluate disruption mitigation investments in the supply chain. *Eur. J. Oper. Res.* 274 (2), 516–530.
- Sy, C.L., Ubando, A.T., Aviso, K.B., Tan, R.R., 2018. Multi-objective target oriented robust optimization for the design of an integrated biorefinery. *J. Clean. Prod.* 170, 496–509.
- Taherkhani, G., Alumur, S.A., Hosseini, M., 2021. Robust stochastic models for profit-maximizing hub location problems. *Transport. Sci.* 55 (6), 1322–1350.
- Tay, D.H., Ng, D.K., Tan, R.R., 2013. Robust optimization approach for synthesis of integrated biorefineries with supply and demand uncertainties. *Environ. Prog. Sustain. Energy* 32 (2), 384–389.
- Torroba, A., Productivo, D., 2020. Atlas de los Biocombustibles Líquidos 2019-2020.
- Wheeler, J., Páez, M.A., Guillén-Gosálbez, G., Mele, F.D., 2018. Combining multi-attribute decision-making methods with multi-objective optimization in the design of biomass supply chains. *Comput. Chem. Eng.* 113, 11–31.
- Zailan, R., Lim, J.S., Manan, Z.A., Alwi, S.R.W., Mohammadi-ivatloo, B., Jamaluddin, K., 2021. Malaysia scenario of biomass supply chain-cogeneration system and optimization modeling development: a review. *Renew. Sustain. Energy Rev.* 148, 111289.
- Zarei, M., Shams, M.H., Niaz, H., Won, W., Lee, C.-J., Liu, J.J., 2022. Risk-based multistage stochastic mixed-integer optimization for biofuel supply chain management under multiple uncertainties. *Renew. Energy* 200, 694–705.
- Zhang, Y., Jiang, Y., 2017. Robust optimization on sustainable biodiesel supply chain produced from waste cooking oil under price uncertainty. *Waste Manag.* 60, 329–339.
- Zhao, K., Ng, T.S., Tan, C.H., Pang, C.K., 2021. An almost robust model for minimizing disruption exposures in supply systems. *Eur. J. Oper. Res.* 295 (2), 547–559.